

# Sex differences, asymmetry and age-related white matter development in infants and 5-year-olds as assessed with Tract-Based Spatial Statistics

Authors: Venla Kumpulainen<sup>a</sup>, Harri Merisaari<sup>a,b</sup>, Eero Silver<sup>a</sup> #, Anni Copeland<sup>a</sup> #, Elmo P. Pulli<sup>a</sup> #, John D Lewis<sup>c</sup>, Ekaterina Saukko<sup>b</sup>, Satu J. Shulist<sup>a</sup>, Jani Saunavaara<sup>d</sup>, Riitta Parkkola<sup>a,b</sup>, Tuire Lähdesmäki<sup>a,e</sup>, Linnea Karlsson<sup>a,f,g,h</sup>, Hasse Karlsson<sup>a,g,h</sup>, Jetro J. Tuulari<sup>a,g,h,i,j</sup>

# shared contribution

- a FinnBrain Birth Cohort Study, Turku Brain and Mind Center, Department of Clinical Medicine, University of Turku, Turku, Finland
- b Department of Radiology, Turku University Hospital, Turku, Finland
- c Montreal Neurological Institute, McGill University, Montreal, Canada
- d Department of Medical Physics, Turku University Hospital and University of Turku, Turku Finland
- e Department of Pediatric Neurology, Turku University Hospital, University of Turku, Turku, Finland
- f Department of Paediatrics and Adolescent Medicine, Turku University Hospital and University of Turku, Turku, Finland
- g Department of Psychiatry, Turku University Hospital & University of Turku, Turku, Finland
- h Centre for Population Health Research, Turku University Hospital and University of Turku, Turku, Finland
- i Turku Collegium for Science, Medicine and Technology, University of Turku, Turku, Finland
- j Department of Psychiatry, University of Oxford, Oxford, United Kingdom (Sigrid Juselius Fellowship)

Corresponding author

Venla Kumpulainen

Email [veviku@utu.fi](mailto:veviku@utu.fi)

Kiinamylynkatu 10, FinnBrain study,

Medisiina A Building

20520 Turku

ORCID: 0000-0003-3375-5445

Running title: White matter features in young children

## Acknowledgements

Funding: VK was supported by the Finnish Medical Foundation and the Finnish Cultural Foundation. HM was supported by Academy of Finland (#26080983). EPP was supported by Päivikki and Sakari Sohlberg foundation and Juho Vainio Foundation. ES was supported by Juho Vainio foundation, Suomen aivosäätiö and Turunmaan Duodecim-seura. SJS was supported by Juho Vainio Foundation, Maire Taponen Foundation and Finnish State Grants for Clinical Research (ERVA). LK was supported by NARSAD Young Investigator Grant (#1956), Signe and Ane Gyllenberg Foundation, the Academy of Finland (#325292 and #308176) and Finnish State Grants for Clinical Research (ERVA). JJT was supported by the Finnish Medical Foundation, Emil Aaltonen Foundation, Sigrid Juselius Foundation, Hospital District of Southwest Finland State Research Grants, Signe and Ane Gyllenberg Foundation, Alfred Kordelin Foundation, Juho Vainio Foundation.

## Author contributions

VK: data collection (5-year-olds), data pre-processing, formal analyses, writing the manuscript draft. HM: designing data processing pipeline, writing the manuscript. EPP, AC, ES: data collection (5-year-olds), writing the manuscript. JDL and JS: designing the MR acquisition protocol, writing the manuscript. SJS: data collection (infants), writing the manuscript. RP: radiological evaluation of the MR images, writing the manuscript. TL: neurological evaluation of the infants, writing the manuscript. LK and HK: establishing the cohort, building infrastructure for carrying out the study, writing the manuscript. JJT: study conception, funding acquisition, supervision of VK, building the pre-processing pipelines, writing the manuscript.

## Declarations

Ethics approval: The study was approved by the Ethics Committee of the Hospital District of Southwest Finland ((07.08.2018) §330, ETMK: 31/180/2011), and performed in accordance with the Declaration of Helsinki.

Data availability: The Finnish law and ethical permissions do not allow open sharing of the data used in this study, but data access is possible via formal material transfer agreements (MTA). Investigators that wish to access the data are encouraged to contact Principal Investigator of the FinnBrain Birth Cohort study Hasse Karlsson ([hasse.karlsson@utu.fi](mailto:hasse.karlsson@utu.fi)).

Informed consent: Both parents of the participating child signed a written informed consent form. The child assent was assured prior to neuroimaging visits.

Declarations of interest: none

## Abstract

The rapid white matter (WM) maturation of first years of life is followed by slower yet long-lasting development, accompanied by learning of more elaborate skills. By the age of five years, behavioural and cognitive differences between females and males, and functions associated with brain lateralization such as language skills are appearing. Diffusion tensor imaging (DTI) can be used to quantify fractional anisotropy (FA) within the WM and increasing values correspond to advancing brain development. To investigate the normal features of WM development during early childhood, we gathered a DTI data set of 166 healthy infants (mean 3.8 wk, range 2-5wk; 89 males; born on gestational week 36 or later) and 144 healthy children (mean 5.4 years, range 5.1-5.8 years; 76 males). The sex differences, lateralization patterns and age-dependent changes were examined using tract-based spatial statistics (TBSS). In 5-year-olds, females showed higher FA in wide-spread regions in the posterior and the temporal WM and more so in the right hemisphere, while sex differences were not detected in infants. Gestational age showed stronger association with FA values compared to age after birth in infants. Additionally, child age at scan associated positively with FA around the age of 5 years in the body of corpus callosum, the connections of which are important especially for sensory and motor functions. Lastly, asymmetry of WM microstructure was detected already in infants, yet significant changes in lateralization pattern seems to occur during early childhood, and in 5-year-olds the pattern already resembles adult-like WM asymmetry.

**Keywords:** white matter, development, TBSS, DTI, sex differences, asymmetry

## Highlights

- White matter tract integrity shows widespread sex differences at the age of 5 years.
- White matter structure is highly lateralized during early childhood, and changes in asymmetry occur between the birth and 5 years of age.
- The white matter lateralization pattern of 5-year-olds, unlike of infants, resembles asymmetry observed in adults.

## 1 Introduction

White matter (WM) microstructural development is linear during prenatal period<sup>1</sup> and continues throughout the childhood with widespread increase in fractional anisotropy (FA) and corresponding decrease in mean diffusivity (MD)<sup>2-14</sup>. The remodelling follows specific trajectories with both regional and temporal variation reflecting the concomitant maturation of motor, behavioural, and cognitive skills.

Generally, postnatal brain development advances with posterior-to-anterior and central-to-peripheral, non-linear patterns<sup>2</sup> and continues from the second trimester into adulthood. Especially rapid developmental period occurs during the first two years of life, when myelination and pruning of axonal connections are driving the increase in WM integrity<sup>3,15,16</sup>. The myelination mainly limits the diffusion perpendicular to the axon axis, which is detected as decreasing radial diffusivity<sup>17</sup> and concomitantly increasing FA values during the development<sup>2-5,8-12,16,18-31</sup>. Commissural and projection fibres, including corpus callosum and pyramidal tracts, are first to reach the adult-like integrity before school-age<sup>10,12,26,32</sup>. These tracts are related to improvement of both gross and fine motors skills, which are prerequisites for further learning of more elaborate skills like writing<sup>33,34</sup><sup>35</sup>. Subsequently, the connections from occipital and limbic areas, associated with e.g. the development of language skills, mature between ages five to eight years<sup>36-38</sup>, followed by the maturation of fronto-temporal association tracts, related to higher-order functions<sup>39-44</sup>, with prolonged development continuing to early adulthood<sup>10</sup>. However, the exact timing of changes especially in young children is still partly elusive and warrants further study.

The developmental patterns of WM show sexual dimorphism with earlier maturation detected in females<sup>32,44-47</sup>, yet more rapid and longer-lasting age-dependent increases in FA in males contributes to levelling off the differences by the age between 10 and 14 years<sup>47</sup>. The studies have provided varying results on the divergence of the trajectories, both in the timing and tract-specific features (Table 1). In two studies, sex differences were already detected during neonatal age<sup>48,49</sup>, even though the differences were limited to few areas. In a sample of 25 infants, males had lower FA in right corticospinal tract<sup>48</sup>, and in another study of age range 0 to 2 years<sup>28</sup>, females showed higher FA in the right sensory and the right uncinate tracts and lower FA in the arcuate and motor tracts. Differences in WM development between females and males were detected in multiple study populations of

older children and adolescents<sup>21,32,45,46,50</sup>, and more specifically between the ages of two and eight years<sup>10</sup>. On the other hand, no developmental sex differences were detected in some studies with wide age ranges<sup>14,26,51,52</sup>. Furthermore, part of the studies have shown FA values in specific tracts (e.g. in the corticospinal tract (CST)<sup>10,21,32,46</sup>) to be higher in males during childhood, in contrast to generally lower FA values detected in males. Additionally, the lateralization of WM microstructure is well-acknowledged both during the brain development<sup>19,29,30,51,53</sup> and adulthood<sup>37,54–57</sup>. Asymmetry of WM tract diffusion properties has been shown to emerge as early as during neonatal age<sup>58</sup>, and is associated with later development of, e.g., language skills<sup>59</sup> but is a relatively understudied topic.

Sex differences in emotional processing<sup>60,61</sup>, personality features<sup>62,63</sup>, temperament<sup>64–66</sup> and behaviour<sup>67,68</sup> are widely reported during childhood and adolescence. Additionally, prevalence of certain diseases is related to sex, e.g., females show more internalizing symptoms and associated disorders such as anxiety<sup>69,70</sup> while incidence of antisocial behaviour<sup>71</sup> and diagnosis of attention deficit hyperactivity disorder (ADHD)<sup>72,73</sup> are overrepresented in males. Unravelling sex-associated features of brain structure and function provide important knowledge on the factors inducing these sex-specific cognitive patterns. Furthermore, alterations in WM lateralization have been associated with conditions such as autism<sup>74</sup> and ADHD<sup>75</sup>. Distinguishing normal variability of WM lateralization might open up new venues for characterizing also disease-associated changes.

Here, we describe sex differences, lateralization patterns, and developmental changes of the brain WM microstructure in populations of infants and 5-year-olds. We hypothesized to find higher FA values in females, positive association between FA values and age, and leftward asymmetry in both age groups based on prior literature.

## 2 Materials and methods

This study was reviewed and approved by the Ethics Committee of the Hospital District of Southwest Finland ((07.08.2018) §330, ETMK: 31/180/2011), and performed in accordance with the Declaration of Helsinki.

## 2.1 Participants

The study included two subpopulations of families recruited as a part of FinnBrain Birth Cohort <sup>76</sup> to brain magnetic resonance imaging (MRI). Twenty-two subjects were included in both subpopulations (10 males). The exclusion criteria of both subpopulations were set to screen healthy participants with no acknowledged developmental problems. The first subpopulation of 190 infants (age of 11 to 54 days from birth at scan, mean 27, SD 7.9; 103 males and 87 females) participated in brain MR scanning between December 2012 and January 2016. The exclusion criteria for infants were: 1) Birth before gestational week (gwk) 36, 2) birth weight of less than 2500g, 3) Apgar score < 5 at 5 minutes after birth, 4) previously diagnosed central nervous system anomaly, an abnormal MRI finding in any previous MRI scan or severe perinatal complication with neurological consequences.

The MR scans of 203 5-year-olds were performed between October 2017 and March 2021. The participants were healthy, normally developing children aged from 5.1 to 5.8 years (mean 5.4, SD 0.11, 111 males, 92 females, 182 right-handed, 14 left-handed, 7 with no preference). The exclusion criteria, in addition to general MRI contraindications, were the following: 1) Birth before gwk 35 (before gwk 32 for separate nested cohort with exposure to synthetic glucocorticoids during pregnancy), 2) major developmental disorder, 3) other types of long-term diagnosis that requires constant contact to hospital, 4) sensory abnormalities (e.g. blindness or deafness), 5) use of daily, regular medication (asthma inhalers during infections was not an exclusion criterium; and desmopressin (®Minirin) medication was allowed), 6) head trauma requiring inpatient care (reported by parents). The informed consent was collected from both parents.

## 2.2 MR imaging

Data acquisition was conducted in Turku University Hospital with a Siemens Magnetom Verio 3T scanner (12-element head/neck matrix coil) for infants and with a Siemens Magnetom Skyra fit 3T scanner (20-element head/neck matrix coil) for 5-year-olds. The scanner was upgraded in between the two data collections. The Generalized Autocalibrating Partially Parallel Acquisition (GRAPPA) technique was used to accelerate imaging. Diffusion weighted imaging protocol was applied with a standard twice-refocused Spin Echo-Echo Planar Imaging (SE-EPI): TR (time of repetition)/TE (time of echo) = 8500/90.0ms (for infants)

and 9300/87.0ms (for 5-year-olds), FOV (field of view) = 208mm, isotropic voxels with 2.0x2.0x2.0mm resolution, b value 1000s/mm<sup>2</sup>, 96 noncollinear diffusion gradient directions divided into three scanning sets (31, 32, and 33 directions) with 9 b0 images (3 b0 = 0s/mm<sup>2</sup> volumes scattered at the beginning, middle and the end of the set). The scan visits included also structural and functional MRI scans<sup>77</sup>, but the current study uses only the structural diffusion data.

The infants were imaged during natural sleep after being fed by (breast) milk. A vacuum mattress was used to reduce movement during the imaging. Soft mouldable silicone ear plugs and hearing muffs were used for hearing protection. Infant MR images included 12 subjects with incidental findings (mainly small subdural hemorrhages), which were handled according to the procedure described in our earlier work<sup>78</sup> and were regarded not to affect the results.

The imaging visit of 5-year-olds was preceded by a home visit to provide detailed information on the study and a home practice period. The imaging session was also simulated before scanning, including practices of lying still and learning how to communicate during imaging. All children were imaged awake or during natural sleep. For more detailed description of the whole image set, the practice period and the imaging visit, see the previous published studies<sup>77,79,80</sup>.

### 2.3 Data analysis

DTI data acquisition was successful with 169 infants and with 163 5-year-olds. We used default settings in DTIprep denoising, slice-wise intensity checking, interlace-wise venetian blind artefact setting, and baseline averaging prior to porting the denoised and cleaned data for tensor fitting with FSL tools (<https://nitrc.org/projects/dtiprep/><sup>81</sup>). As the applied settings were detected to pass volumes with motion-related artifacts, all volumes were manually inspected and the ones with residual artifacts were excluded. For subsequent analysis, 30 directions were chosen per subject by maximizing the angular resolution, and subjects with insufficient number of directions after quality control steps were excluded<sup>82</sup>. We chose to use 30 directions, as in our previous study<sup>79</sup> we observed that increasing the number of diffusion-encoding directions over 18 provided no additional advantage in repeatability of results. Further, inclusion of more directions would have led to a decrease in

the sample size. With this choice, the final number of subjects was 166 infants (89 males, 77 females) and 144 5-year-olds (76 males, 68 females).

Pre-processing of quality-controlled data was conducted with FSL 6.0 (FMRIB software library, University of Oxford, UK). b0 images, including at least one image per imaging set, were co-registered and averaged (FLIRT, FMRIB's Linear Image Registration Tool), and the brain mask was created with Brain Extraction Tool (BET version 1.0.0)<sup>83</sup> with settings -R -f 0.3. Motion and eddy current correction were performed with FSL tools with concurrent rotation of the b vector matrix. The scalar maps were computed with FSL's dtifit. Tract-based spatial statistics (TBSS) pipeline of FSL<sup>84</sup> was used to estimate WM tract skeletons with the following settings (5-year-olds/infants): "tbss\_2\_reg" flag -T/-t (target being a study-specific template), "tbss\_3\_postreg" flag -S, FA threshold 0.2/0.15. Relative residual rotational and translational framewise displacements were measured to quantify the intrascanner head motion. The used pipelines have been thoroughly validated, please see more detailed description of data analysis pipeline, test-retest reliability, and assessment of optimal number of diffusion-encoding directions to DTI scalars in our previously published articles<sup>79,82,85</sup>.

General linear model (GLM) with FSL's randomise tool was used for voxel-wise analysis of inter-subject variation. In the infant group, sex, age from birth and gestational age, rotational and translational mean framewise displacement measures (to control intrascanner head motion), maternal pre-pregnancy body mass index (BMI), birth weight, maternal smoking during pregnancy, and maternal socio-economic status (SES; evaluated by educational level and categorized into two classes: 1. low [elementary school] and medium [high school or occupational education], 2. high [examination from university or university for applied sciences]) were explored as independent contributors. For 5-year-olds, sex, age at scan, handedness, rotational and translational mean framewise displacement measures, maternal pre-pregnancy BMI, ponderal index, maternal smoking during pregnancy and maternal SES were explored as independent contributors. The analyses were conducted with 5000 permutations and multiple comparison correction with threshold-free cluster enhancement (TFCE; corrected  $p < 0.05$  regarded as statistically significant). As the age and sex showed statistically significant correlations with FA, further analyses were performed with age and sex as main variables and other variables as covariates.



Sensitivity analyses with gestational age (birth before gestational week 35 for 5-year-olds), maternal pre-pregnancy BMI, maternal age at birth, maternal SES, smoking during pregnancy, prenatal exposure to corticosteroids or selective serotonin/serotonin-noradrenaline reuptake inhibitors (SSRI/SNRI) during pregnancy, and maternal perinatal depressive/anxiety symptoms (Edinburgh Postnatal Depressive Scale (EPDS)<sup>86</sup> and Symptom Checklist (SCL-90)<sup>87</sup>) at 2<sup>nd</sup> trimester and three months postpartum (for 5-year-olds) were conducted. See the supplementary material for demographical information and regression analysis workflow (Supplement Tables 1 and 2).

Additionally, we examined the lateralization patterns of FA by FSL's "tbss\_sym" both over all participants and separately in females and males. Lateralization was estimated by subtracting the right-sided FA values from the left-side ones, followed by a "one-sample t test" randomise analysis (5000 permutations, TFCE correction) to detect areas with significant variation. The mean image and standard deviation (SD) of lateralized values was calculated with fslmaths. Tract-wise mean FA values were extracted with coregistration of JHU Neonate atlas<sup>88</sup> for infants and JHU-ICBM-DTI atlas<sup>89</sup> for 5-year-olds to the TBSS skeleton images.

Statistical analyses for tract-wise extracted mean FA values were performed with SPSS version 27.0 (IBM Corp. 2020, Armonk, NY, USA). Tract-wise sex differences were estimated with independent samples t test (two-tailed), and asymmetric differences with one-sample t test, with Bonferroni corrected p value thresholded at 0.001 (0.05/36 tracts). Effect sizes for group differences were estimated with Cohen's d. Comparison between asymmetries in a subcohort of 22 infants and 5-year-olds was conducted with paired t test with Bonferroni corrected p value threshold at 0.002 (0.05/22).

## 3 Results

### 3.1 Sex differences

#### 3.1.1 Infants

Sex showed no statistically significant correlation with FA values in the infants after controlling for age at scan and gestational age, intrascanner head motion, birth weight, maternal BMI, SES, and smoking.

### 3.1.2 Five-year-olds

A significant effect of sex on FA values was detected in widespread regions at the age of five years, and was statistically strongest in posterior and temporal parts, and in the right hemisphere (Figure 1). Females had higher FA values in all regions with significant difference, i.e. no regions with higher FA in males were detected. The results remained significant after controlling for gestational age, handedness, ponderal index, intrascanner head motion, smoking during pregnancy, pre-pregnancy BMI, and SES. In sensitivity analyses, the pattern of results in TBSS remained similar and statistically significant (data not shown). Group differences of whole WM tract mean FA values between females and males are provided in Supplement Table 3.

**Figure 1.** Sex-differences with tract-based spatial statistics (TBSS) at the age of 5 years. Higher fractional anisotropy (FA) values detected in females are present in widely distributed areas, especially in posterior and right hemisphere regions. Regions with statistically significant difference showed in 3D (top left corner) and in axial plane (bottom left), threshold-free cluster enhancement (TFCE) correction applied, regression with 5000 permutations,  $p < 0.05$  (red colour bar showing p values), age as a covariate. Additionally, on the right, group-differences in mean FA across whole tract between females (F) and males (M) showed in splenium of corpus callosum (SCC; Cohen's d 0.48), right retrolenticular internal capsule (rl IC; Cohen's d 0.58), left inferior longitudinal fasciculus/inferior fronto-occipital fasciculus (ILF/IFOF; Cohen's d 0.58) and left posterior thalamic radiation and optic tract (PTR/OR; Cohen's d 0.66).  $p < 0.005 = *$ ,  $p < 0.001 = **$ . R = right, L = left

## 3.2 Age effects

### 3.2.1 Infants

The gestational age showed wide statistically significant positive correlations ( $p < 0.01$ ) with FA values after controlling for age from birth and sex (Figure 2; results with  $p < 0.05$  in the Supplement Figure 1). Additionally, age from birth showed positive correlations with FA values ( $p < 0.05$ ) after controlling for the gestational age and sex. The effect of gestational age on FA values was greater compared to the effects detected after birth. The results remain significant after controlling for intrascanner head motion, prenatal exposure to

smoking, maternal age, pre-pregnancy BMI and SES. The covariates included in the sensitivity analyses did not affect the results. We inspected the age effects also separately in females and males and observed no difference in association between gestational age and FA after controlling for age after birth or other covariates between males and females. When inspected separately, the age after birth and FA showed positive association in males ( $p < 0.05$  after controlling for covariates), but the result did not remain statistically significant in females.

**Figure 2.** Effect of the age (controlled with gestational age) and the gestational age (controlled with age after birth) on fractional anisotropy (FA) with tract-based spatial statistics (TBSS) in infants. Positive correlation between both ages and FA are detected, with stronger and wider correlation between gestational age and FA. TFCE (threshold-free cluster enhancement) correction applied, 5000 permutations,  $p < 0.05$  (for age from birth) and  $p < 0.001$  (for gestational age), blue colour bar showing p value. R = right, L = left.

### 3.2.2 Five-year-olds

Within our age range of 5.1 to 5.8 years, the age was positively correlated with FA values in the body of corpus callosum (BCC) (Figure 3). After controlling for maternal pre-pregnancy BMI, maternal age, SES, and exposure to tobacco smoking during pregnancy, the result did not remain significant (TFCE corrected  $p < 0.06$ , with which also an additional cluster in left frontal area was observed; See Supplement Figure 2). When examined separately, no significant age-effects were found in males, and in females the effect in BCC did not reach statistical significance ( $p = 0.08$ ).

**Figure 3.** Effect of the age on fractional anisotropy (FA) with tract-based spatial statistics (TBSS) around the age of 5 years. Positive correlation between age and FA of corpus callosum is detected. TFCE (threshold-free cluster enhancement) correction applied, 5000 permutations,  $p < 0.05$  (red-yellow colour bar showing p value), age as a covariate. P = posterior, A = anterior, R = right, L = left.

### 3.3 Lateralization

### 3.3.1 Infants

Lateralization of brain WM was detected in infants in multiple tracts. Leftward lateralized WM regions are depicted in Figure 4 (TFCE corrected  $p < 0.01$ ; results with  $p < 0.05$  in the Supplement Figure 3). Sex was not observed to affect the lateralization pattern.

**Figure 4.** Lateralization pattern of white matter tract fractional anisotropy (FA) with tract-based spatial statistics (TBSS) in infants. Significant regions with leftward asymmetry in blue. Threshold-free cluster enhancement (TFCE) correction applied, 5000 permutations,  $p < 0.01$  (blue colour bar showing  $p$  value). R = right, L = left, A = anterior, P = posterior. Tracts are marked with white circles. Additionally, left-right difference (left minus right, negative values denote rightward asymmetry) of FA in uncinate (UNC), anterior limb of internal capsule (ALIC), posterior limb of internal capsule (PLIC), thalamic radiation/optic tract (PTR/OR), posterior and superior corona radiata (PCR and SCR), and the statistical significance with one-sample  $t$  test and effect sizes.

### 3.3.2 Five-year-olds

The WM structure was highly lateralized at the age of five years (Figure 5). Statistically significantly higher FA values in left-sided tracts were detected in multiple areas (e.g. frontal and temporal areas and in midbrain; TFCE corrected  $p < 0.001$  in Figure 5 and with  $p < 0.05$  in the Supplement Figure 4). The mean image of lateralization pattern (Supplement Figures 5 and 6) indicating the magnitude and direction (left/rightward) of the hemispheric asymmetry of FA values also shows rightward lateralized regions, for example, in the anterior limb of internal capsule (ALIC) and antero-lateral corpus callosum. Leftward asymmetry was detected, for example, in cingulate, inferior fronto-occipital fasciculus, posterior corpus callosum, fronto-parietal region, and midbrain. In most of the WM tracts, both leftward and rightward lateralized subregions were observed. Inter-subject variation of FA asymmetry was detected to be emphasized to peripheral WM tract regions (Supplement Figure 7 shows the SD of lateralization pattern). Tract-wise lateralized FA (left-right) and effect sizes for the differences between whole tract mean FA values are provided in Supplement Table 4. Statistically significant differences in the asymmetry pattern were not observed between females and males (Supplement Figure 8 shows sex-specific left-right lateralization patterns).

**Figure 5.** Lateralization pattern of white matter (WM) tract fractional anisotropy (FA) with tract-based spatial statistics (TBSS) around the age of 5 years. Significant regions with leftward asymmetry in red, threshold-free cluster enhancement (TFCE) correction applied, 5000 permutations,  $p < 0.001$  (red colour bar showing p value). R = right, L = left. Specified tracts are marked with white circles. Additionally, left-right difference (left minus right, negative values denote rightward asymmetry) of FA in cingulum (CING), uncinate (UNC), anterior limb of internal capsule (ALIC), external capsule (EC), posterior thalamic radiation/optic tract (PTR/OR), superior fronto-occipital fasciculus (SFOF), anterior and superior corona radiata (ACR and SCR), and the statistical significance with one-sample t test and effect sizes.

Differences in left-right lateralization of WM tracts between infants and 5-year-olds was compared in subset of 22 subjects included in both age groups (Figure 6). The detected asymmetries were more distinct in 5-year-olds, and the direction of asymmetry did not remain similar in all tracts from birth to the age of 5 years. Leftward asymmetries were detected in both age groups in superior longitudinal fasciculus (SLF), cingulum (CING), and cingulate (CG) and rightward asymmetry, for example, in the ALIC. However, the initial rightward asymmetry of posterior limb of internal capsule (PLIC), corticospinal tracts (CST), and inferior longitudinal fasciculus/inferior fronto-occipital fasciculus (ILF/IFOF), was revealed to shift to leftward laterality. A similar pattern was detected when repeating the comparison with entire subpopulations of infants ( $N = 166$ ) and 5-year-olds ( $N = 144$ ). In the group of 22 that were included in both the infant cohort and the 5-year-olds, the difference between lateralized FA in infants and 5-year-olds were statistically significant ( $p < 0.002$ ) for CST, PLIC, anterior corona radiata and CG. Mean FA values of each tract in infants and in 5-year-olds are provided in the Supplement Table 5.

**Figure 6.** Left-right asymmetries of white matter (WM) tract fractional anisotropy (FA) values in infants and in 5-year-olds, measured from left-right tract-based spatial statistics (TBSS) skeleton by extracting with JHU-ICBM Atlas. Subpopulation of 22 subjects with MR scanning both at 2-5 weeks after birth and at age of 5 years. Positive values denote for leftward and negative values for rightward asymmetry. UNC = uncinata, SFOF = superior fronto-occipital fasciculus, SLF = superior longitudinal fasciculus, ST = stria terminalis, CING = cingulum, CG = cingulate, EC = external capsule, ILF/IFOF = inferior longitudinal fasciculus/inferior fronto-occipital fasciculus, PTR (OR) = posterior thalamic radiation (optic tract), PCR = posterior corona radiata, SCR = superior corona radiata, ACR = anterior corona radiata, rLIC = retrolenticular internal capsule, PLIC = posterior limb of internal capsule, ALIC = anterior limb of internal capsule, sup = superior, inf = inferior, cereb = cerebellar, CST = corticospinal tract, SCC = splenium of corpus callosum, BCC = body of corpus callosum, GCC = genu of corpus callosum, PCT = pontine crossing tract, MCP = middle cerebellar peduncle.

## 4 Discussion

We found widespread sex differences in white matter FA values in our sample of healthy, typically developing ca. 5-year-olds. Females had higher FA in all areas with significant differences, which were widely scattered throughout WM tracts. Sex differences were not detected in infants. Additionally, significant hemispheric asymmetries of FA values were observed in multiple WM tracts both in infants and at the age of 5 years. Hemispheric lateralization pattern was detected not to stay stable from birth to the age of 5 years. Lastly, age was positively associated with FA values during 6<sup>th</sup> year of life in mid-posterior part of the corpus callosum.

Sex differences in WM tract structure were expected based on prior studies (Table 1). The previous literature on sex difference during development is, however, inconclusive, as the age ranges, methods and results vary widely between studies. In part of prior studies, no sex differences were observed<sup>14,51,52</sup>, and in longitudinal developmental studies the observed sex differences have argued to be minor<sup>19,26</sup>. In the current study, the differences were significantly wider than previously described, and higher FA in females was observed in all regions with differences. The result highlights the sexual dimorphism in brain structure during development with significant detectable differences in multiple regions at the age of five years. Instead of tract-specific differences detected in a part of previous studies, we

detected FA values to be higher in females across all brain regions. One possible explanation for varying results in prior literature may be the transient dynamics of sex differences. In studies reporting higher FA values in specified tracts in males<sup>21,32,46</sup> the age ranges are also higher (from 8 years onwards). The WM development of males has been shown to proceed later but also with steeper rates achieving and, in part of tracts, outpacing females<sup>10</sup>. A large cohort of 9- to 65-year-old subjects also showed sex differences to diminish with age<sup>90</sup>, further explaining why differences might not have been observed in older samples. Widespread sex differences observed in our 5-year-old population were emphasized to the posterior and temporal parts of the brain and were statistically more significant in the right hemisphere. These results agree with the prior studies showing both earlier brain development in females<sup>18,32,44-47</sup> and developmental pattern of maturation progressing in posterior-to-anterior direction. Our result of higher FA in females in widespread regions provides new insight into the timing of sex-dependent WM development trajectories and implies that at the age of 5 years the WM integrity is higher in females.

Hemispheric asymmetries of WM microstructure appear early<sup>58</sup> and are also suggested to remain stable throughout the brain development<sup>30,91</sup>. However, asymmetries in WM of healthy, normally-developing children are not inspected carefully across whole WM, even though alterations of asymmetry is associated with different conditions such as dyslexia<sup>59</sup>. Knowledge of normal variation in asymmetric WM features is an important prerequisite for making conclusions from alterations in asymmetry. One recent study by Stephens et al. has shown significant asymmetry in all WM regions inspected (arcuate, cingulum, uncinate, IFOF, ILF, SLF and SCC) during the first 6 years of life<sup>30</sup>. Other studies on WM asymmetries in pediatric populations have mainly focused on age groups over 5 years of age, the sample sizes have remained quite modest and mainly leftward laterality in limited WM tracts has been observed<sup>19,29,51,92,93</sup>. Our findings further consolidate the emergence of hemispheric asymmetries during WM development. Lateralization patterns were detected already during neonatal ages, but also changes in asymmetric WM structure were detected between birth and the age of 5 years. The pattern of 5-year-olds resembled considerably the WM asymmetry detected in adult population. We compared our results with two prior adult-population studies (Supplement Figure 9), a TBSS study by Takao et al.<sup>91</sup> and a Fixel-Based Analysis (FBA) study by Honnedevasathana Arun et al. 2021<sup>94</sup>. However, according to our

results, some alterations in asymmetric pattern seem to occur between neonatal period and the age of 5 years. In comparison to prior longitudinal study of 0 to 6-year-olds<sup>30</sup>, in which the lateralization was measured based on mean DTI indices of each tract, we also detected variation in asymmetry within the tracts. Mainly leftward lateralization of CG was repeated in our population, however, the asymmetries of certain WM tracts varied between infants and 5-year-olds suggesting further development of the lateralization pattern during first years of life. Similarly, as in prior adult-studies<sup>57,94</sup>, we did not find association between the lateralization pattern and sex. Taken together, these findings highlight the role of asymmetry in fundamental structure of WM and underline the importance of early childhood as an essential period in the appearance of diverging lateralization patterns that may contribute to variation in cognitive measures and executive functions<sup>95</sup>, language development<sup>96</sup> and to predisposition to diseases such as ADHD<sup>97</sup> and autism<sup>74,98</sup>.

Age from birth and gestational age were expectedly detected to correlate positively with FA values. Gestational age showed stronger correlation with FA after controlling for the age from birth, which is plausible given the extensive WM development and partial myelination already *in utero*. When inspected separately, age after birth showed significant positive association with FA in males but not in females. The result may partly stem from different sample sizes (89 males vs 77 females) and is addressed for future longitudinal studies with more optimal data for observing developmental changes. Also, significant positive correlation between the age and FA of BCC was detected even in a narrow age range between 5.1 and 5.8 years. The posterior BCC and the isthmus of CC contain the primary somatosensory and motor fibres<sup>99</sup>, and the finding of rapid increase in the integrity in this area at the age of five years may be related to, e.g. the concurrent development of motor skills and bimanual movements<sup>34,100</sup>. Previously, higher initial FA values of callosal fibres have been associated with lower increase rates after the age of two years compared to for example association tracts<sup>10</sup>. One explanatory factor for detecting distinct age-effect in our data specifically in the CC might be the highly uniform organization of callosal fibres rendering the area susceptible for finding group differences if they exist.

The current study has also some limitations. The sample size is acknowledged to be modest, and the results need to be repeated in larger population and in other ethnic groups. As there were only 22 subjects included in both subpopulations, and the MR scanner was



updated between imaging, the study setting is not technically longitudinal, but the subpopulations are considered as separate groups.

## 5 Conclusions

Rapid increase of the WM integrity, i.e. increase in FA values, occurs during the first five years of life. At that developmental timing, broad sex differences in WM structure are observed: higher FA and thus presumably more advanced development is detected in multiple regions in females compared to males. Additionally, the WM structure is widely lateralized during early development, and at the age of five years the lateralization pattern resembles considerably the ones previously described in adult studies, which has clear differences to those observed in infants.

## References

1. Wilson S, Pietsch M, Cordero-Grande L, et al. Development of human white matter pathways in utero over the second and third trimester. *Proc Natl Acad Sci U S A*. 2021;118(20):1-7. doi:10.1073/pnas.2023598118
2. Krogsrud SK, Fjell AM, Tamnes CK, et al. Changes in white matter microstructure in the developing brain — A longitudinal diffusion tensor imaging study of children from 4 to 11 years of age. *Neuroimage*. 2016;124:473-486. doi:10.1016/j.neuroimage.2015.09.017
3. Hermoye L, Saint-Martin C, Cosnard G, et al. Pediatric diffusion tensor imaging: Normal database and observation of the white matter maturation in early childhood. *Neuroimage*. 2006;29(2):493-504. doi:10.1016/j.neuroimage.2005.08.017
4. Lebel C, Deoni S. The development of brain white matter microstructure. *Neuroimage*. 2018;182(June 2017):207-218. doi:10.1016/j.neuroimage.2017.12.097
5. Lebel C, Treit S, Beaulieu C. A review of diffusion MRI of typical white matter development from early childhood to young adulthood. *NMR Biomed*. 2017;(October 2016):1-23. doi:10.1002/nbm.3778
6. Löbel U, Sedlacik J, Güllmar D, Kaiser WA, Reichenbach JR, Mentzel HJ. Diffusion tensor imaging: The normal evolution of ADC, RA, FA, and eigenvalues studied in multiple anatomical regions of the brain. *Neuroradiology*. 2009;51(4):253-263. doi:10.1007/s00234-008-0488-1
7. McGraw P, Liang L, Provenzale JM. Evaluation of normal age-related changes in anisotropy during infancy and childhood as shown by diffusion tensor imaging. *American Journal of Roentgenology*. 2002;179(6):1515-1522. doi:10.2214/ajr.179.6.1791515

8. Muftuler LT, Poggi E, Buss C, et al. Development of white matter pathways in typically developing preadolescent children. *Brain Res.* 2012;1466:33-43. doi:10.1016/j.brainres.2012.05.035
9. Qiu D, Tan LH, Zhou K, Khong PL. Diffusion tensor imaging of normal white matter maturation from late childhood to young adulthood: Voxel-wise evaluation of mean diffusivity, fractional anisotropy, radial and axial diffusivities, and correlation with reading development. *Neuroimage.* 2008;41(2):223-232. doi:10.1016/j.neuroimage.2008.02.023
10. Reynolds JE, Grohs MN, Dewey D, Lebel C. Global and regional white matter development in early childhood. *Neuroimage.* 2019;196(April):49-58. doi:10.1016/j.neuroimage.2019.04.004
11. Rollins NK, Glasier P, Seo Y, Morriss MC, Chia J, Wang Z. Age-related variations in white matter anisotropy in school-age children. *Pediatr Radiol.* 2010;40:1918-1930. doi:10.1007/s00247-010-1744-1
12. Tamnes CK, Østby Y, Fjell AM, Westlye LT, Due-Tønnessen P, Walhovd KB. Brain maturation in adolescence and young adulthood: Regional age-related changes in cortical thickness and white matter volume and microstructure. *Cerebral Cortex.* 2010;20(3):534-548. doi:10.1093/cercor/bhp118
13. Taki Y, Thyreau B, Hashizume H, et al. Linear and curvilinear correlations of brain white matter volume, fractional anisotropy, and mean diffusivity with age using voxel-based and region-of-interest analyses in 246 healthy children. *Hum Brain Mapp.* 2013;34(8):1842-1856. doi:10.1002/hbm.22027
14. Uda S, Matsui M, Tanaka C, et al. Normal development of human brain white matter from infancy to early adulthood: A diffusion tensor imaging study. *Dev Neurosci.* 2015;37(2):182-194. doi:10.1159/000373885
15. Huang H, Zhang J, Wakana S, et al. White and gray matter development in human fetal, newborn and pediatric brains. *Neuroimage.* 2006;33(1):27-38. doi:10.1016/j.neuroimage.2006.06.009
16. Dubois J, Dehaene-Lambertz G, Kulikova S, Poupon C, Hüppi PS, Hertz-Pannier L. The early development of brain white matter: A review of imaging studies in fetuses, newborns and infants. *Neuroscience.* 2014;276:48-71. doi:10.1016/j.neuroscience.2013.12.044
17. Song SK, Sun SW, Ramsbottom MJ, Chang C, Russell J, Cross AH. Demyelination revealed through MRI as increased radial (but unchanged axial) diffusion of water. *Neuroimage.* 2002;17(3):1429-1436. doi:10.1006/nimg.2002.1267
18. Barnea-Goraly N, Menon V, Eckert M, et al. White matter development during childhood and adolescence: A cross-sectional diffusion tensor imaging study. *Cerebral Cortex.* 2005;15(12):1848-1854. doi:10.1093/cercor/bhi062
19. Bonekamp D, Nagae LM, Degaonkar M, et al. Diffusion Tensor Imaging in Children and Adolescents: Reproducibility, Hemispheric, and Age-Related Differences. *Neuroimage.* 2007;34(2):733-742.
20. Chen Z, Zhang H, Yushkevich PA, Liu M, Beaulieu C. Maturation along white matter tracts in human brain using a diffusion tensor surface model tract-specific analysis. *Front Neuroanat.* 2016;10(9):1-18. doi:10.3389/fnana.2016.00009

21. Clayden JD, Jentschke S, Muñoz M, et al. Normative development of white matter tracts: Similarities and differences in relation to age, gender, and intelligence. *Cerebral Cortex*. 2012;22(8):1738-1747. doi:10.1093/cercor/bhr243
22. Colby JB, Van Horn JD, Sowell ER. Quantitative in vivo evidence for broad regional gradients in the timing of white matter maturation during adolescence. *Neuroimage*. 2011;54(1):25-31. doi:10.1016/j.neuroimage.2010.08.014
23. Gao W, Lin W, Chen Y, et al. Temporal and spatial development of axonal maturation and myelination of white matter in the developing brain. *AJNR*. Published online 2009. doi:10.1038/jid.2014.371
24. Genc S, Malpas CB, Gulenc A, et al. Longitudinal patterns of white matter fibre density and morphology in children are associated with age and pubertal stage. *Dev Cogn Neurosci*. 2020;45:100853. doi:10.1016/j.dcn.2020.100853
25. Huang H, Shu N, Mishra V, et al. Development of Human Brain Structural Networks Through Infancy and Childhood. 2015;(May):1389-1404. doi:10.1093/cercor/bht335
26. Lebel C, Walker L, Leemans A, Phillips L, Beaulieu C. Microstructural maturation of the human brain from childhood to adulthood. 2008;40:1044-1055. doi:10.1016/j.neuroimage.2007.12.053
27. Moon W jin, Provenzale J, Sarikaya B, et al. Diffusion Tensor Imaging Assessment of White Matter Maturation in Childhood and Adolescence. *AJR Am J Roentgenol*. 2011;197(3):704-712. doi:10.2214/AJR.10.6382.
28. Moura L, Kempton M, Barker G, et al. Age-effects in white matter using associated diffusion tensor imaging and magnetization transfer ratio during late childhood and early adolescence. *Magn Reson Imaging*. 2016;34(4):529-534. doi:10.1016/j.mri.2015.12.021
29. Snook L, Paulson LA, Roy D, Phillips L, Beaulieu C. Diffusion tensor imaging of neurodevelopment in children and young adults. *Neuroimage*. 2005;26(4):1164-1173. doi:10.1016/j.neuroimage.2005.03.016
30. Stephens RL, Langworthy BW, Short SJ, Girault JB, Styner MA, Gilmore JH. White matter development from birth to 6 years of age: A longitudinal study. *Cerebral Cortex*. 2020;30(12):6152-6168. doi:10.1093/cercor/bhaa170
31. Uda S, Matsui M, Tanaka C, et al. Normal development of human brain white matter from infancy to early adulthood: A diffusion tensor imaging study. *Dev Neurosci*. 2015;37(2):182-194. doi:10.1159/000373885
32. Asato MR, Terwilliger R, Woo J, Luna B. White matter development in adolescence: A DTI study. *Cerebral Cortex*. 2010;20(9):2122-2131. doi:10.1093/cercor/bhp282
33. Grohs MN, Reynolds JE, Dewey D, Lebel C. Corpus callosum microstructure is associated with motor function in preschool children. *Neuroimage*. 2018;183(September):828-835. doi:10.1016/j.neuroimage.2018.09.004
34. Johansen-Berg H, Della-Maggiore V, Behrens TEJ, Smith SM, Paus T. Integrity of white matter in the corpus callosum correlates with bimanual co-ordination skills. *Neuroimage*. 2007;36(SUPPL. 2). doi:10.1016/j.neuroimage.2007.03.041

35. Sigurdsson E, van Os J, Fombonne E. Are impaired childhood motor skills a risk factor for adolescent anxiety? Results from the 1958 U.K. birth cohort and the National Child Development Study. *American Journal of Psychiatry*. 2002;159(6):1044-1046. doi:10.1176/appi.ajp.159.6.1044
36. Yeatman JD, Dougherty RF, Ben-Shachar M, Wandell BA. Development of white matter and reading skills. *Proc Natl Acad Sci U S A*. 2012;109(44). doi:10.1073/pnas.1206792109
37. Catani M, Allin MPG, Husain M, et al. Symmetries in human brain language pathways correlate with verbal recall. *Proc Natl Acad Sci U S A*. 2007;104(43):17163-17168. doi:10.1073/pnas.0702116104
38. Broce IJ, Bernal B, Altman N, et al. Fiber pathways supporting early literacy development in 5–8-year-old children. *Brain Cogn*. 2019;134(December 2018):80-89. doi:10.1016/j.bandc.2018.12.004
39. Gao W, Zhu H, Lin W. A unified optimization approach for diffusion tensor imaging technique. *Neuroimage*. 2009;44(3):729-741. doi:10.1016/j.neuroimage.2008.10.004
40. Salman L, Aviram A, Krispin E, Wiznitzer A, Chen R, Gabbay-Benziv R. Adverse neonatal and maternal outcome following vacuum-assisted vaginal delivery: does indication matter? *Arch Gynecol Obstet*. 2017;295(5):1145-1150. doi:10.1007/s00404-017-4339-3
41. Poussaint TY, Moeller KK. Imaging of pediatric head trauma. *Neuroimaging Clin N Am*. 2002;12:271-294.
42. Oishi et al. 2013. Quantitative evaluation of brain development using anatomical MRI and diffusion tensor imaging. *Int J Dev Neurosci*. Published online 2013. doi:10.1038/jid.2014.371
43. Hutton JS, Phelan K, Horowitz-Kraus T, et al. Shared Reading Quality and Brain Activation during Story Listening in Preschool-Age Children. *Journal of Pediatrics*. 2017;191:204-211.e1. doi:10.1016/j.jpeds.2017.08.037
44. Simmonds DJ, Hallquist MN, Asato M, Luna B. Developmental stages and sex differences of white matter and behavioral development through adolescence: A longitudinal diffusion tensor imaging (DTI) study. *Neuroimage*. 2014;92:356-368. doi:10.1016/j.neuroimage.2013.12.044
45. Bava S, Boucquey V, Goldenberg D, et al. Sex Differences in Adolescent White Matter Architecture. *Brain Res*. 2011;1375:41-48. doi:10.1016/j.brainres.2010.12.051.
46. Wang Y, Adamson C, Yuan W, et al. Sex differences in white matter development during adolescence: A DTI study. *Brain Res*. 2012;1478(1):1-15. doi:10.1016/j.brainres.2012.08.038
47. Seunarine KK, Clayden JD, Jentschke S, et al. Sexual Dimorphism in White Matter Developmental Trajectories Using Tract-Based Spatial Statistics. *Brain Connect*. 2016;6(1):37-47. doi:10.1089/brain.2015.0340
48. Saadani-Makki F, Hagmann C, Balédent O, Makki MI. Early assessment of lateralization and sex influences on the microstructure of the white matter corticospinal tract in healthy term neonates. *J Neurosci Res*. 2019;97(4):480-491. doi:10.1002/jnr.24359

49. Geng X, Gouttard S, Sharma A, et al. Quantitative Tract-Based White Matter Development from Birth to Age Two Years. *Neuroimage*. 2012;61(3):542-557. doi:10.1016/j.neuroimage.2012.03.057.
50. Lewis JD, Acosta H, Tuulari JJ, et al. Allometry in the corpus callosum in neonates: Sexual dimorphism. *Hum Brain Mapp*. 2022;(May):1-11. doi:10.1002/hbm.25977
51. Eluvathingal TJ, Hasan KM, Kramer L, Fletcher JM, Ewing-Cobbs L. Quantitative diffusion tensor tractography of association and projections fibers in normally developing children and adolescent. *Cerebral Cortex*. 2007;17(12):2760-2768. doi:10.1161/CIRCULATIONAHA.110.956839
52. Muetzel RL, Collins PF, Mueller BA, Schissel AM, Lim KO, Luciana M. The development of corpus callosum microstructure and associations with bimanual task performance in healthy adolescents. *Neuroimage*. 2008;39(4):1918-1925.
53. Lebel C, Beaulieu C. Lateralization of the arcuate fasciculus from childhood to adulthood and its relation to cognitive abilities in children. *Hum Brain Mapp*. 2009;30(11):3563-3573. doi:10.1002/hbm.20779
54. Cao Y, Whalen S, Huang J, Berger KL, DeLano MC. Asymmetry of subinsular anisotropy by in vivo diffusion tensor imaging. *Hum Brain Mapp*. 2003;20(2):82-90. doi:10.1002/hbm.10130
55. Westerhausen R, Huster RJ, Kreuder F, Wittling W, Schweiger E. Corticospinal tract asymmetries at the level of the internal capsule: Is there an association with handedness? *Neuroimage*. 2007;37(2):379-386. doi:10.1016/j.neuroimage.2007.05.047
56. Vernooij MW, Smits M, Wielopolski PA, Houston GC, Krestin GP, van der Lugt A. Fiber density asymmetry of the arcuate fasciculus in relation to functional hemispheric language lateralization in both right- and left-handed healthy subjects: A combined fMRI and DTI study. *Neuroimage*. 2007;35(3):1064-1076. doi:10.1016/j.neuroimage.2006.12.041
57. Takao H, Abe O, Yamasue H, et al. Gray and white matter asymmetries in healthy individuals aged 21-29 years: A voxel-based morphometry and diffusion tensor imaging study. *Hum Brain Mapp*. 2011;32(10):1762-1773. doi:10.1002/hbm.21145
58. Song JW, Mitchell PD, Kolasinski J, Grant PE, Galaburda AM, Takahashi E. Asymmetry of white matter pathways in developing human brains. *Cerebral Cortex*. 2015;25(9):2883-2893. doi:10.1093/cercor/bhu084
59. Banfi C, Koschutnig K, Moll K, Schulte-Körne G, Fink A, Landerl K. White matter alterations and tract lateralization in children with dyslexia and isolated spelling deficits. *Hum Brain Mapp*. 2019;40(3):765-776. doi:10.1002/hbm.24410
60. Else-Quest NM, Higgins A, Allison C, Morton LC. Gender Differences in Self-Conscious Emotional Experience: A Meta-Analysis. *Psychol Bull*. 2012;138(5):947-981. doi:10.1037/a0027930
61. Christov-moore L, Simpson EA, Coudé G, Grigaityte K, Iacoboni M, Francesco P. Neuroscience and Biobehavioral Reviews Empathy: Gender effects in brain and behavior. *Neurosci Biobehav Rev*. 2014;46:604-627. doi:10.1016/j.neubiorev.2014.09.001

62. Schmitt DP, Long AE, Mcphearson A, Brien KO, Remmert B, Shah SH. Personality and gender differences in global perspective. *International Journal of Psychology*. 2017;52:45-56. doi:10.1002/ijop.12265
63. Weinstein A, Dannon P. Is Impulsivity a Male Trait Rather than Female Trait? Exploring the Sex Difference in Impulsivity. *Curr Behav Neurosci Rep*. 2015;2:9-14. doi:10.1007/s40473-015-0031-8
64. Boo GM De, Spiering M. Pre-Adolescent Gender Differences in Associations between Temperament, Coping, and Mood. *Clinical Psychology and Psychotherapy*. 2010;320(November 2009):313-320.
65. Else-quest NM, Hyde JS, Goldsmith HH, Hulle CA Van. Gender Differences in Temperament: A Meta-Analysis. *Psychol Bull*. 2006;132(1):33-72. doi:10.1037/0033-2909.132.1.33
66. Olino TM, Durbin CE, Klein DN, Hayden EP, Dyson MW. Gender differences in young children's temperament traits: Comparisons across observational and parent-report methods. *J Pers*. 2014;81(2):119-129. doi:10.1111/jopy.12000.
67. Hines M. Sex-related variation in human behavior and the brain. *Trends Cogn Sci*. 2010;14(10). doi:10.1016/j.tics.2010.07.005
68. Coe JL, Micalizzi L, Josefson B, Parade SH, Seifer R, Tyrka AR. Sex Differences in Associations between Early Adversity, Child Temperament, and Behavior Problems. *Int J Behav Dev*. 2021;44(6):490-504. doi:10.1177/0165025420912012.
69. Li SH, Graham BM. Why are women so vulnerable to anxiety, trauma-related and stress-related disorders? The potential role of sex hormones. *Lancet Psychiatry*. 2017;4(1):73-82. doi:10.1016/S2215-0366(16)30358-3
70. Alloy LB, Hamilton JL, Hamlat EJ, Abramson LY. Pubertal Development, Emotion Regulatory Styles, and the Emergence of Sex Differences in Internalizing Disorders and Symptoms in Adolescence. *Clin Psychol Sci*. 2017;4(5):867-881. doi:10.1177/2167702616643008
71. Holthausen BS, Habel U. Sex Differences in Personality Disorders. *Curr Psychiatry Rep*. 2018;20. doi:doi.org/10.1007/s11920-018-0975-y
72. Mowlem FD, Rosenqvist MA, Martin J, Lichtenstein P, Asherson P, Larsson H. Sex differences in predicting ADHD clinical diagnosis and pharmacological treatment. *Eur Child Adolesc Psychiatry*. 2019;28(4):481-489. doi:10.1007/s00787-018-1211-3
73. Rucklidge JJ. Gender Differences in Attention-Deficit/Hyperactivity Disorder. *Psychiatr Clin N Am*. 2010;33(2):357-373. doi:10.1016/j.psc.2010.01.006
74. Carper RA, Treiber JM, Yandall DeJesus S, Müller RA. Reduced Hemispheric Asymmetry of White Matter Microstructure in Autism Spectrum Disorder. *J Am Acad Child Adolesc Psychiatry*. 2016;55(12):1073-1080. doi:10.1016/j.jaac.2016.09.491.
75. Silk TJ, Vilgis V, Adamson C, et al. Abnormal asymmetry in frontostriatal white matter in children with attention deficit hyperactivity disorder. *Brain Imaging Behav*. 2016;10(4):1080-1089. doi:10.1007/s11682-015-9470-9
76. Karlsson L, Tolvanen M, Scheinin NM, et al. Cohort Profile: The FinnBrain Birth Cohort Study (FinnBrain). *Int J Epidemiol*. Published online 2017:1-12. doi:10.1093/ije/dyx173

77. Copeland A, Silver E, Korja R, et al. Infant and Child MRI: A Review of Scanning Procedures. *Front Neurosci.* 2021;15(July):1-16. doi:10.3389/fnins.2021.666020
78. Kumpulainen V, Lehtola SJ, Tuulari JJ, et al. Prevalence and Risk Factors of Incidental Findings in Brain MRIs of Healthy Neonates—The FinnBrain Birth Cohort Study. *Front Neurol.* 2020;10(January). doi:10.3389/fneur.2019.01347
79. Kumpulainen V, Merisaari H, Copeland A, et al. Effect of number of diffusion encoding directions in Diffusion Metrics of 5-year-olds using Tract-Based Spatial Statistical analysis. *Eur J Neurosci.* Published online July 2022. doi:10.1111/ejn.15785
80. Pulli EP, Silver E, Kumpulainen V, et al. Feasibility of FreeSurfer Processing for T1-Weighted Brain Images of 5-Year-Olds: Semiautomated Protocol of FinnBrain Neuroimaging Lab. *Front Neurosci.* 2022;16(May):1-20. doi:10.3389/fnins.2022.874062
81. Oguz I, Farzinfar M, Matsui J, et al. DTIPrep: Quality control of diffusion-weighted images. *Front Neuroinform.* 2014;8(JAN):1-11. doi:10.3389/fninf.2014.00004
82. Merisaari H, Tuulari JJ, Karlsson L, et al. Test-retest reliability of Diffusion Tensor Imaging metrics in neonates. *Neuroimage.* 2019;197(April):598-607. doi:10.1016/j.neuroimage.2019.04.067
83. Smith SM. Fast robust automated brain extraction. *Hum Brain Mapp.* 2002;17(3):143-155. doi:10.1002/hbm.10062
84. Smith SM, Jenkinson M, Johansen-Berg H, et al. Tract-based spatial statistics: Voxelwise analysis of multi-subject diffusion data. *Neuroimage.* 2006;31(4):1487-1505. doi:10.1016/j.neuroimage.2006.02.024
85. Nolvi S, Tuulari JJ, Lavonius T, et al. Newborn white matter microstructure moderates the association between maternal postpartum depressive symptoms and infant negative reactivity. *Soc Cogn Affect Neurosci.* 2020;15(6):649-660. doi:10.1093/scan/nsaa081
86. Cox JL, Holden JM, Sagovsky R. Detection of Postnatal Depression: Development of the 10-item Edinburgh Postnatal Depression scale. *British Journal of Psychiatry.* 1987;150(JUNE):782-786. doi:10.1192/bjp.150.6.782
87. Holi MM, Samallahti PR, Aalberg VA. A Finnish validation study of the SCL-90. *Acta Psychiatr Scand.* 1998;97(1):42-46. doi:10.1111/j.1600-0447.1998.tb09961.x
88. Oishi K, Mori S, Donohue PK, et al. Multi-contrast human neonatal brain atlas: Application to normal neonate development analysis. *Neuroimage.* 2011;56(1):8-20. doi:10.1016/j.neuroimage.2011.01.051
89. Mori S, Oishi K, Jiang H, et al. Stereotaxic white matter atlas based on diffusion tensor imaging in an ICBM template. *Neuroimage.* 2008;40(2):570-582. doi:10.1016/j.neuroimage.2007.12.035
90. Seitz J, Cetin-Karayumak S, Lyall A, et al. Investigating Sexual Dimorphism of Human White Matter in a Harmonized, Multisite Diffusion Magnetic Resonance Imaging Study. *Cerebral Cortex.* 2021;31(1):201-212. doi:10.1093/cercor/bhaa220

91. Takao H, Hayashi N, Ohtomo K. White matter asymmetry in healthy individuals: A diffusion tensor imaging study using tract-based spatial statistics. *Neuroscience*. 2011;193:291-299. doi:10.1016/j.neuroscience.2011.07.041
92. Verhoeven JS, Sage CA, Leemans A, et al. Construction of a stereotaxic DTI atlas with full diffusion tensor information for studying white matter maturation from childhood to adolescence using tractography-based segmentations. *Hum Brain Mapp*. 2010;31(3):470-486. doi:10.1002/hbm.20880
93. Wilde EA, McCauley SR, Chu Z, et al. Diffusion tensor imaging of hemispheric asymmetries in the developing brain. *J Clin Exp Neuropsychol*. 2009;31(2):205-218. doi:10.1080/13803390802098118
94. Honnedevashtana Arun A, Connelly A, Smith RE, Calamante F. Characterisation of white matter asymmetries in the healthy human brain using diffusion MRI fixel-based analysis. *Neuroimage*. 2021;225(November 2020):117505. doi:10.1016/j.neuroimage.2020.117505
95. Yin X, Han Y, Ge H, et al. Inferior frontal white matter asymmetry correlates with executive control of attention. *Hum Brain Mapp*. 2013;34(4):796-813. doi:10.1002/hbm.21477
96. O'Muircheartaigh J, Dean DC, Dirks H, et al. Interactions between white matter asymmetry and language during neurodevelopment. *Journal of Neuroscience*. 2013;33(41):16170-16177. doi:10.1523/JNEUROSCI.1463-13.2013
97. Yin X, Han Y, Ge H, et al. Inferior frontal white matter asymmetry correlates with executive control of attention. *Hum Brain Mapp*. 2013;34(4):796-813. doi:10.1002/hbm.21477
98. Liu J, Tsang T, Jackson L, et al. Altered Lateralization of Dorsal Language Tracts in 6-Week-Old Infants at Risk for Autism. *Dev Sci*. 2019;22(3). doi:10.1111/desc.12768
99. Fabri M, Pierpaoli C, Barbaresi P, Polonara G. Functional topography of the corpus callosum investigated by DTI and fMRI. *World J Radiol*. 2014;6(12):895-906. doi:10.4329/wjr.v6.i12.895
100. Grohs MN, Reynolds JE, Dewey D, Lebel C. Corpus callosum microstructure is associated with motor function in preschool children. *Neuroimage*. 2018;183(September):828-835. doi:10.1016/j.neuroimage.2018.09.004
101. Herting MM, Maxwell EC, Irvine C, Nagel BJ. The impact of sex, puberty, and hormones on white matter microstructure in adolescents. *Cerebral Cortex*. 2012;22(9):1979-1992. doi:10.1093/cercor/bhr246
102. Schmithorst VJ, Holland SK, Dardzinski BJ. Developmental differences in white matter architecture between boys and girls. *Hum Brain Mapp*. Published online 2008. doi:10.1161/CIRCULATIONAHA.110.956839



Table 1. Literature review of white matter sex differences in age groups close to our study. TBSS = tract-based spatial statistics, TBA = tract-based analysis, ROI = region of interest, FA = fractional anisotropy, MD = mean diffusivity, RD = radial diffusivity, AD = axial diffusivity, CST = corticospinal tract, IC = internal capsule, SLF = superior longitudinal fasciculus, IFOF = inferior fronto-occipital fasciculus, ILF = inferior longitudinal fasciculus, SCP = superior cerebral peduncle, PLIC = posterior limb of internal capsule, UNC = uncinate fasciculus, AF = arcuate fasciculus, BCC = body of corpus callosum, GCC = genu of corpus callosum, SCC = splenium of corpus callosum

Author Year Journal	Age (years)	Sample size	Method	Main finding
Seunarine et al. 2016 Brain Connectivity	8-16	53	TBSS	<ul style="list-style-type: none"> <li>○ Females: ↑FA in females</li> <li>○ Males: ↑MD in males in majority of tracts (e.g. bilateral CST, IC, EC, thalamic radiation, SLF, left cingulum)</li> </ul>
Asato et al. 2010 Cerebral Cortex	8-28	114	TBSS	<ul style="list-style-type: none"> <li>○ Earlier maturation in females (RD)</li> <li>○ Females: only right frontal SLF continued to mature after adolescence</li> <li>○ Males: most tracts continued to develop into adulthood (exception: right SLF and IFOF)</li> </ul>
Bava et al. 2011 Brain Research	12-14	58	TBSS	<ul style="list-style-type: none"> <li>○ Females: ↑FA in right SCR and bilateral CST + ↓MD in right ILF and left forceps major</li> <li>○ Males: ↑AD in right SLF, ILF and forceps minor</li> </ul>
Herting et al. 2012 Cerebral Cortex <sup>101</sup>	10-16	77	TBSS	<ul style="list-style-type: none"> <li>○ Males: ↑FA in all regions analysed (SCP, PLIC, IFOF, midbrain, cingulum)</li> </ul>
Geng et al. 2012	0-2	211	Tractography TBA	<ul style="list-style-type: none"> <li>○ Females: ↑FA in right sensory tract + ↑AD in right UNC</li> <li>○ Males: ↑AD in right AF and right motor tracts</li> </ul>

<hr/>				
NeuroImage				
Reynolds et al. 2019	2-8	120	Tractography	<ul style="list-style-type: none"> <li>○ Earlier development in females, faster and greater development in males</li> <li>○ Females: ↓ global MD and ↓ MD in BCC, fornix, ILF and SLF + faster ↑ FA in CST</li> <li>○ Males: ↑ FA in GCC and CST + faster ↓ MD in fornix, ILF and SLF</li> </ul>
NeuroImage				
Lebel et al. 2011	5-32	103	Tractography	<ul style="list-style-type: none"> <li>○ Females: ↑ FA in SCC</li> <li>○ Males: ↑ FA in cingulum, bilateral CST, SLF, UNC</li> </ul>
The Journal of Neuroscience				
Eluvathingal et al. 2007	6-17	31	Tractography	<ul style="list-style-type: none"> <li>○ Females: ↓ RD in bilateral ILF and right IFOF</li> </ul>
Cerebral Cortex				
Clayden et al. 2012	8-16	59	Tractography	<ul style="list-style-type: none"> <li>○ Males: faster decrease of MD (higher initial values, cross during development)</li> </ul>
Cerebral Cortex				
Schmithorst et al. 2008	5-18	106	ROI	<ul style="list-style-type: none"> <li>○ Females: ↑ FA in SCC + ↑ MD in right occipito-parietal and superior part of CST <ul style="list-style-type: none"> <li>○ Positive correlation between age and right frontal/occipito-temporal FA</li> <li>○ Negative correlation between age and left frontal FA</li> </ul> </li> <li>○ Males: ↑ FA in frontal regions, in right AF and in left parietal and occipito-parietal WM + ↑ MD in right CST and frontal WM <ul style="list-style-type: none"> <li>○ Positive correlation between age and frontal FA</li> <li>○ Negative correlation between age and right AF FA</li> </ul> </li> </ul>
Human Brain Mapping <sup>102</sup>				
Muetzel et al. 2008	9-24	92	ROI	<ul style="list-style-type: none"> <li>○ No sex difference in FA or MD values detected in corpus callosum</li> </ul>
NeuroImage				
<hr/>				

Supplementary material to

## Sex differences, asymmetry and age-related white matter development in infants and 5-year-olds as assessed with Tract-Based Spatial Statistics

Authors: Venla Kumpulainen<sup>a</sup>, Harri Merisaari<sup>a,b</sup>, Eero Silver<sup>a</sup> #, Anni Copeland<sup>a</sup> #, Elmo P. Pulli<sup>a</sup> #, John D Lewis<sup>c</sup>, Ekaterina Saukko<sup>b</sup>, Satu J. Shulist<sup>a</sup>, Jani Saunavaara<sup>d</sup>, Riitta Parkkola<sup>a,b</sup>, Tuire Lähdesmäki<sup>a,e</sup>, Linnea Karlsson<sup>a,f,g,h</sup>, Hasse Karlsson<sup>a,g,h</sup>, Jetro J. Tuulari<sup>a, g,h,i,j</sup>

# shared contribution

- k FinnBrain Birth Cohort Study, Turku Brain and Mind Center, Department of Clinical Medicine, University of Turku, Turku, Finland
- l Department of Radiology, Turku University Hospital, Turku, Finland
- m Montreal Neurological Institute, McGill University, Montreal, Canada
- n Department of Medical Physics, Turku University Hospital and University of Turku, Turku Finland
- o Department of Pediatric Neurology, Turku University Hospital, University of Turku, Turku, Finland
- p Department of Paediatrics and Adolescent Medicine, Turku University Hospital and University of Turku, Turku, Finland
- q Department of Psychiatry, Turku University Hospital & University of Turku, Turku, Finland
- r Centre for Population Health Research, Turku University Hospital and University of Turku, Turku, Finland
- s Turku Collegium for Science, Medicine and Technology, University of Turku, Turku, Finland
- t Department of Psychiatry, University of Oxford, Oxford, United Kingdom (Sigrid Juselius Fellowship)

Corresponding author

Venla Kumpulainen

Email [veviku@utu.fi](mailto:veviku@utu.fi)

Kiinamylynkatu 10, FinnBrain study,

Medisiina A Building

20520 Turku

ORCID: 0000-0003-3375-5445

**Supplement Table 1.** Demographics of the study population. SD = standard deviation, gwk = gestational week, BMI = body-mass index, SSRI/SNRI = selective serotonin/serotonine-noradrenaline re-uptake inhibitor, EPDS = Edinburgh postnatal depressive scale, SCL = symptom checklist, mm = millimetre

<b>Demographics</b>	Infants (N = 166)	5-year-olds (N = 144)
Females (%)	77 (46)	68 (47)
Males (%)	89 (54)	76 (53)
Age (years) (SD, range)		5.38 (0.11; 5.09-5.79)
Gestational age < 35 gwk (%)	0	1 (0.69)
Gestational age at birth, days (SD, range)	279 (8.3; 265-296)	
Gestational age at scan, days (SD, range)	305 (7.2; 291-325)	
Handedness (%)		
Right		127 (88)
Left		12 (8.3)
Both		3 (2.1)
NA		2 (1.4)
At birth (SD, range)		
Weight (g)	3530 (448; 2530-4700)	3530 (520; 1790-4980)
Height (cm)	50.4 (1.88; 44-56)	50.4 (2.48; 43-56)
At the imaging (SD, range)		
Weight (kg)		21.1 (3.02; 14.0-31.0)
Height (cm)		114 (4.59; 100-125)
Ponderal index (kg/m <sup>3</sup> )		14.0 (1.28; 11.0-18.0)
Maternal (SD, range)		
Pre-pregnancy BMI (kg/m <sup>2</sup> )	24.4 (4.18; 17.5-40.8)	24.2 (4.10; 17.5-36.7)
NA (%)	3 (1.8)	1 (0.69)
Age at birth	30.0 (4.3; 19-41)	30.4 (4.8; 18-41)
Exposure during pregnancy (%)		
Tobacco smoking (yes/no/NA)	9(5.4)/153(92)/4(2.4)	8(5.5)/134(93)/2(1.4)
SSRI/SNRI	11(6.6)/147(89)/8(4.8)	6(4.2)/128(89)/10(6.9)
Glucocorticosteroids	8(4.8)/144(87)/14(8.4)	14(9.7)/130(90)/0
Depressive/anxiety symptoms (SD, range)		
EPDS, 2 <sup>nd</sup> trimester	5.19 (5.05; 0-25.0)	4.80 (4.22; 0-21.0)
EPDS, 3 months postpartum		4.26 (3.90; 0-19.0)
SCL-90 sum, 2 <sup>nd</sup> trimester	4.12 (5.11; 0-28.0)	3.62 (3.75; 0-19.0)
SCL-90 sum, 3 months postpartum		2.55 (3.50; 0-17.0)
Frame-wise head displacement		
Mean rotational (°; SD, range)	0.30 (0.22; 0.06-1.64)	0.18 (0.08; 0.06-0.56)
Mean translational (mm; SD, range)	1.88 (0.48-6.61; 0.87)	1.16 (0.27; 0.64-2.26)

**Supplement Table 2.** Description of regression and sensitivity analyses in the current study.

BMI = body-mass index, SES = socio-economic status, SSRI/SNRI = selective serotonin/serotonin-noradrenaline re-uptake inhibitor, EPDS = Edinburgh postnatal depressive scale, SCL = symptom checklist

Regression analyses	Main variables	Covariates used in sensitivity analyses
5-year-olds	<ul style="list-style-type: none"><li>• sex</li><li>• age</li><li>• handedness</li><li>• Ponderal index</li><li>• Maternal pre-pregnancy BMI</li><li>• Maternal socio-economic status (by educational status, categorised)</li></ul>	<ul style="list-style-type: none"><li>• Gestational age</li><li>• Maternal age at birth</li><li>• Maternal pre-pregnancy BMI</li><li>• Maternal SES</li><li>• Smoking during pregnancy</li><li>• Exposure to glucocorticosteroids during pregnancy</li></ul>

	<ul style="list-style-type: none"> <li>high/medium to low)</li> <li>Smoking during pregnancy</li> <li>Intrascanner head motion</li> </ul>	<ul style="list-style-type: none"> <li>Exposure to SSRI/SNRI during pregnancy</li> <li>EPDS at 2<sup>nd</sup> trimester</li> <li>EPDS 3 months postpartum</li> <li>SCL-90 at 2<sup>nd</sup> trimester</li> <li>SCL-90 3 months postpartum</li> </ul>
Infants	<ul style="list-style-type: none"> <li>Age from birth</li> <li>Gestational age</li> <li>Sex</li> <li>Birth weight</li> <li>Maternal pre-pregnancy BMI</li> <li>Maternal socio-economic status</li> <li>Smoking during pregnancy</li> <li>Intrascanner head motion</li> </ul>	<ul style="list-style-type: none"> <li>Gestational age</li> <li>Age from birth</li> <li>Maternal age at birth</li> <li>Maternal pre-pregnancy BMI</li> <li>Maternal SES</li> <li>Smoking during pregnancy</li> <li>Exposure to glucocorticosteroids during pregnancy</li> <li>Exposure to SSRI/SNRI during pregnancy</li> <li>EPDS at 2<sup>nd</sup> trimester</li> <li>SCL-90 at 2<sup>nd</sup> trimester</li> </ul>

#### Example of sensitivity analyses

Basic model	FA = age + sex + maternal BMI
Sensitivity model 1	FA = age + sex + maternal BMI + maternal age
Sensitivity model 2	FA = age + sex + maternal BMI + SES
Sensitivity model 3	FA = age + sex + maternal BMI + smoking
Sensitivity model ...	FA = age + sex + maternal BMI + ...

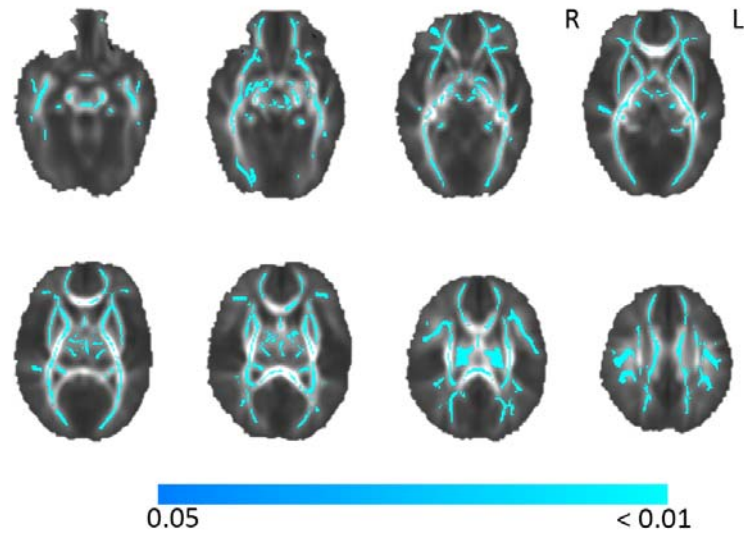
**Supplement Table 3.** Mean fractional anisotropy (FA) and standard deviation (SD) of each white matter tract and differences between girls and boys. CST = corticospinal tract, ML = medial lemniscus, ICP = inferior cerebellar peduncle, SCP = superior cerebellar peduncle, CP = cerebral peduncle, ALIC = anterior limb of internal capsule, PLIC = posterior limb of internal capsule, ACR = anterior corona radiata, SCR = superior corona radiata, PCR = posterior corona radiata, PTR (OR) = posterior thalamic radiation (optic tract), ILF/IFOF = inferior longitudinal fasciculus/inferior fronto-occipital fasciculus, EC = external capsule, CG = cingulate, CING = cingulum, ST = stria terminalis, SLF = superior longitudinal fasciculus, SFOF = superior fronto-occipital fasciculus, UNC = uncinata. Left-right difference of mean FA provided, negative values denote for rightward lateralization. Statistical significance calculated with independent sample t test (two-tailed), Bonferroni corrected p value = 0.001 (0.05/36), tracts with significant difference in bold.

		Mean			Cohen's d
		FA	SD	Sig.	
<b>Right</b>	<b>girl</b>	<b>0,587</b>	<b>0,029</b>	<b>0,000</b>	<b>0,680</b>
<b>PTR/OR</b>	<b>boy</b>	<b>0,566</b>	<b>0,032</b>		
<b>Left</b>	<b>girl</b>	<b>0,587</b>	<b>0,030</b>	<b>0,000</b>	<b>0,658</b>
<b>PTR/OR</b>	<b>boy</b>	<b>0,566</b>	<b>0,034</b>		
<b>Right</b>	<b>girl</b>	<b>0,516</b>	<b>0,028</b>	<b>0,000</b>	<b>0,644</b>
<b>ILF/IFOF</b>	<b>boy</b>	<b>0,499</b>	<b>0,026</b>		

		Mean				
		FA	SD	Sig.	Cohen's d	
SCC	girl	0,748	0,025	0,005	0,482	
	boy	0,735	0,029			
GCC	girl	0,719	0,033	0,694	0,066	
	boy	0,721	0,036			
BCC	girl	0,633	0,038	0,470	0,121	
	boy	0,637	0,037			
fornix	girl	0,450	0,041	0,253	0,192	
	boy	0,442	0,043			
Right CST	girl	0,488	0,024	0,666	0,072	
	boy	0,487	0,028			
Left CST	girl	0,504	0,027	0,288	0,178	
	boy	0,509	0,028			
Right ALIC	girl	0,544	0,023	0,725	0,059	
	boy	0,543	0,025			
Left ALIC	girl	0,523	0,023	0,519	0,108	
	boy	0,520	0,027			
Right PLIC	girl	0,654	0,020	0,570	0,095	
	boy	0,652	0,020			
Left PLIC	girl	0,657	0,021	0,952	0,010	
	boy	0,657	0,021			
<b>Right rLIC</b>	<b>girl</b>	<b>0,553</b>	<b>0,028</b>	<b>0,001</b>	<b>0,582</b>	
	boy	0,538	0,026			
Left rLIC	girl	0,569	0,024	0,007	0,458	
	boy	0,559	0,023			
Right ACR	girl	0,458	0,028	0,150	0,242	
	boy	0,452	0,028			
Left ACR	girl	0,452	0,028	0,049	0,331	
	boy	0,443	0,027			
Right SCR	girl	0,471	0,024	0,120	0,261	
	boy	0,464	0,025			
Left SCR	girl	0,478	0,024	0,854	0,031	
	boy	0,477	0,022			
Right PCR	girl	0,444	0,025	0,056	0,321	
	boy	0,436	0,028			
Left PCR	girl	0,441	0,030	0,414	0,137	
	boy	0,437	0,027			

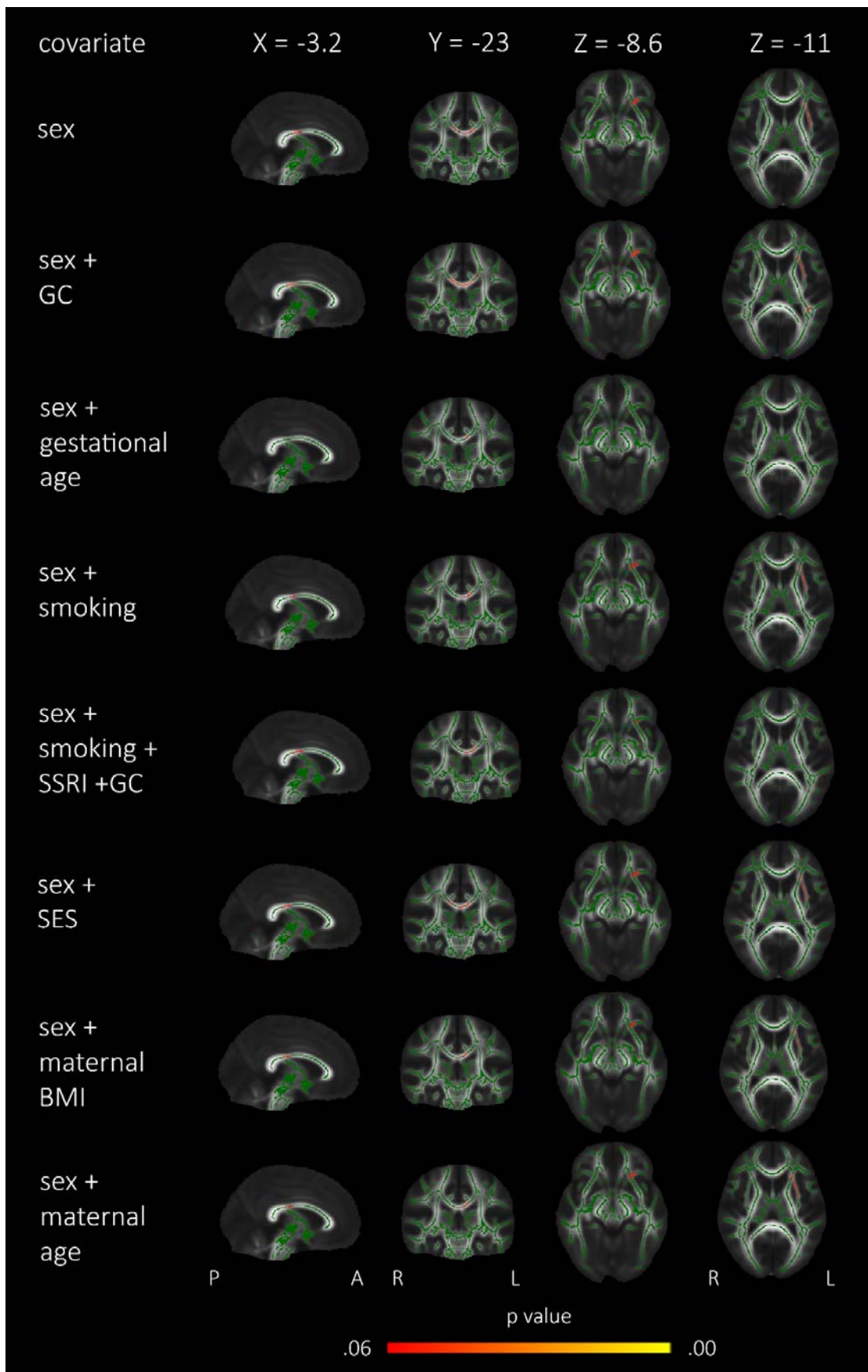
  

<b>Left ILF/IFOF</b>	<b>girl</b>	<b>0,517</b>	<b>0,026</b>	<b>0,001</b>	<b>0,579</b>
	<b>boy</b>	<b>0,502</b>	<b>0,026</b>		
Right EC	girl	0,381	0,020	0,311	0,170
	boy	0,377	0,023		
Left EC	girl	0,400	0,025	0,773	0,048
	boy	0,401	0,020		
Right CING	girl	0,458	0,035	0,463	0,123
	boy	0,462	0,038		
Left CING	girl	0,483	0,035	0,453	0,126
	boy	0,488	0,039		
Right CG	girl	0,409	0,039	0,860	0,029
	boy	0,408	0,037		
Left CG	girl	0,406	0,036	0,269	0,185
	boy	0,412	0,037		
Right Fornix/ST	girl	0,506	0,026	0,851	0,031
	boy	0,505	0,032		
Left Fornix/ST	girl	0,521	0,025	0,955	0,009
	boy	0,521	0,032		
Right SLF	girl	0,476	0,029	0,014	0,416
	boy	0,465	0,025		
Left SLF	girl	0,477	0,029	0,097	0,279
	boy	0,469	0,025		
Right SFOF	girl	0,478	0,036	0,469	0,121
	boy	0,473	0,041		
Left SFOF	girl	0,446	0,037	0,709	0,062
	boy	0,449	0,045		
Right UNC	girl	0,445	0,030	0,031	0,364
	boy	0,434	0,028		
Left UNC	girl	0,453	0,035	0,194	0,218
	boy	0,447	0,028		

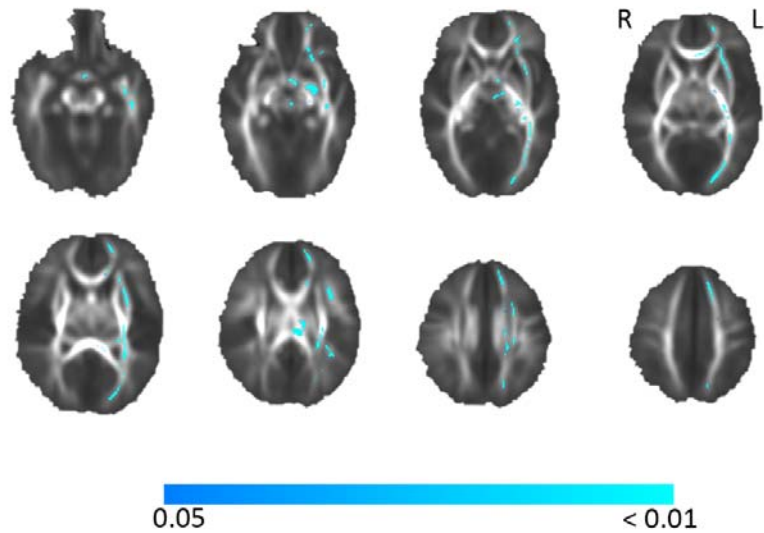


**Supplement Figure 1.** Effect of gestational age on fractional anisotropy analysed voxel-wise with tract-based spatial statistics with covariates (age after birth, sex, birth weight, intrascanner head motion, maternal tobacco smoking during pregnancy, socioeconomic status (low-medium/high), maternal pre-pregnancy body-mass index). Analysis conducted with 5000 permutations, threshold-free cluster enhancement correction applied,  $p < 0.05$ , R = right, L = left.

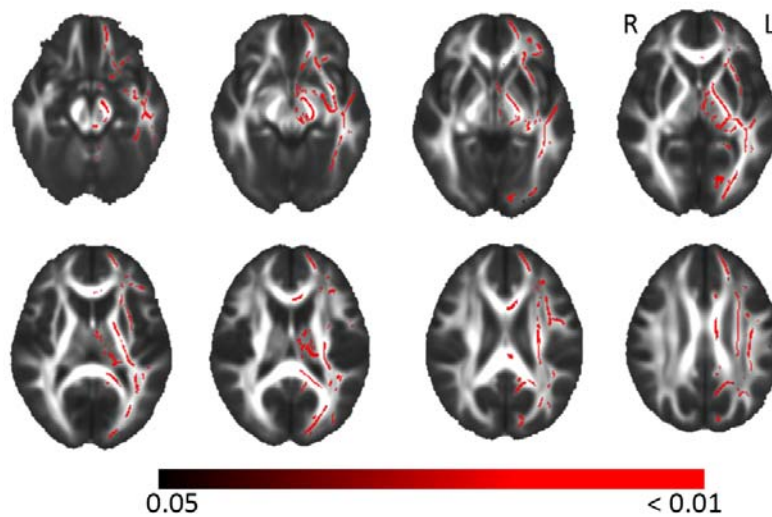




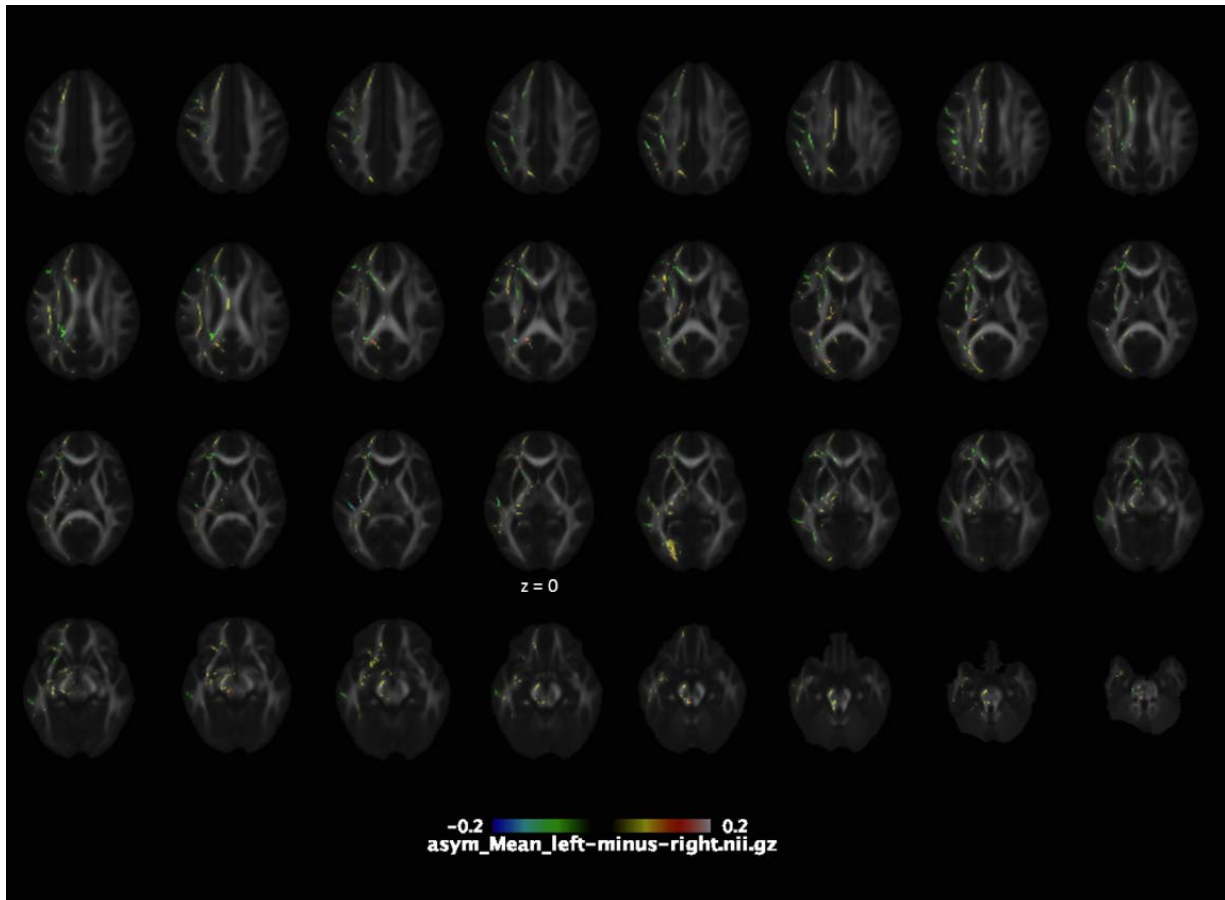
**Supplement Figure 2.** Age-effects analysed voxel-wise with tract-based spatial statistics with covariates (prenatal glucocorticoid (GC) exposure, gestational age, maternal tobacco smoking during pregnancy, exposure to selective serotonin reuptake inhibitors (SSRI) during pregnancy, socioeconomic status (SES; low-medium/high), maternal pre-pregnancy bodymass index (BMI) and maternal age at birth ). Analyses conducted with 5000 permutations, TFCE (threshold-free cluster enhancement) correction applied,  $p < 0.06$ .



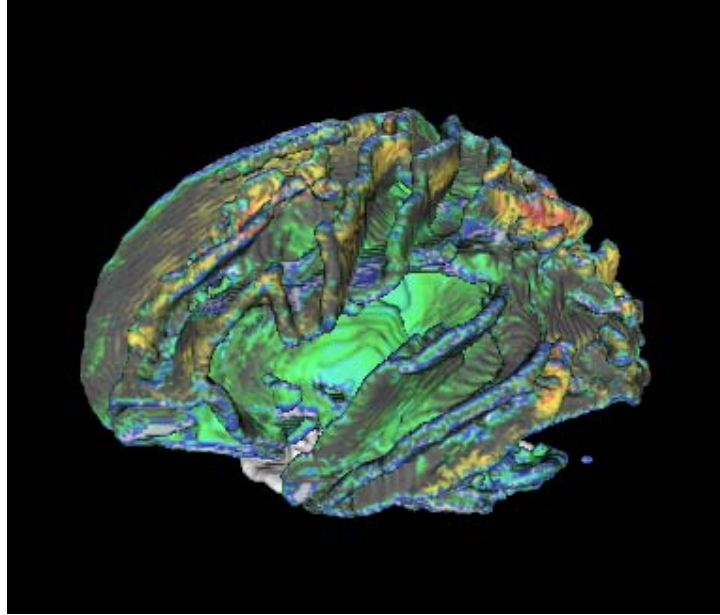
**Supplement Figure 3.** Lateralization pattern of white matter tract fractional anisotropy with tract-based spatial statistics in infants. Significant regions with leftward asymmetry in blue. Threshold-free cluster enhancement (TFCE) correction applied, 5000 permutations,  $p < 0.05$  (blue colour bar showing  $p$  value). R = right, L = left



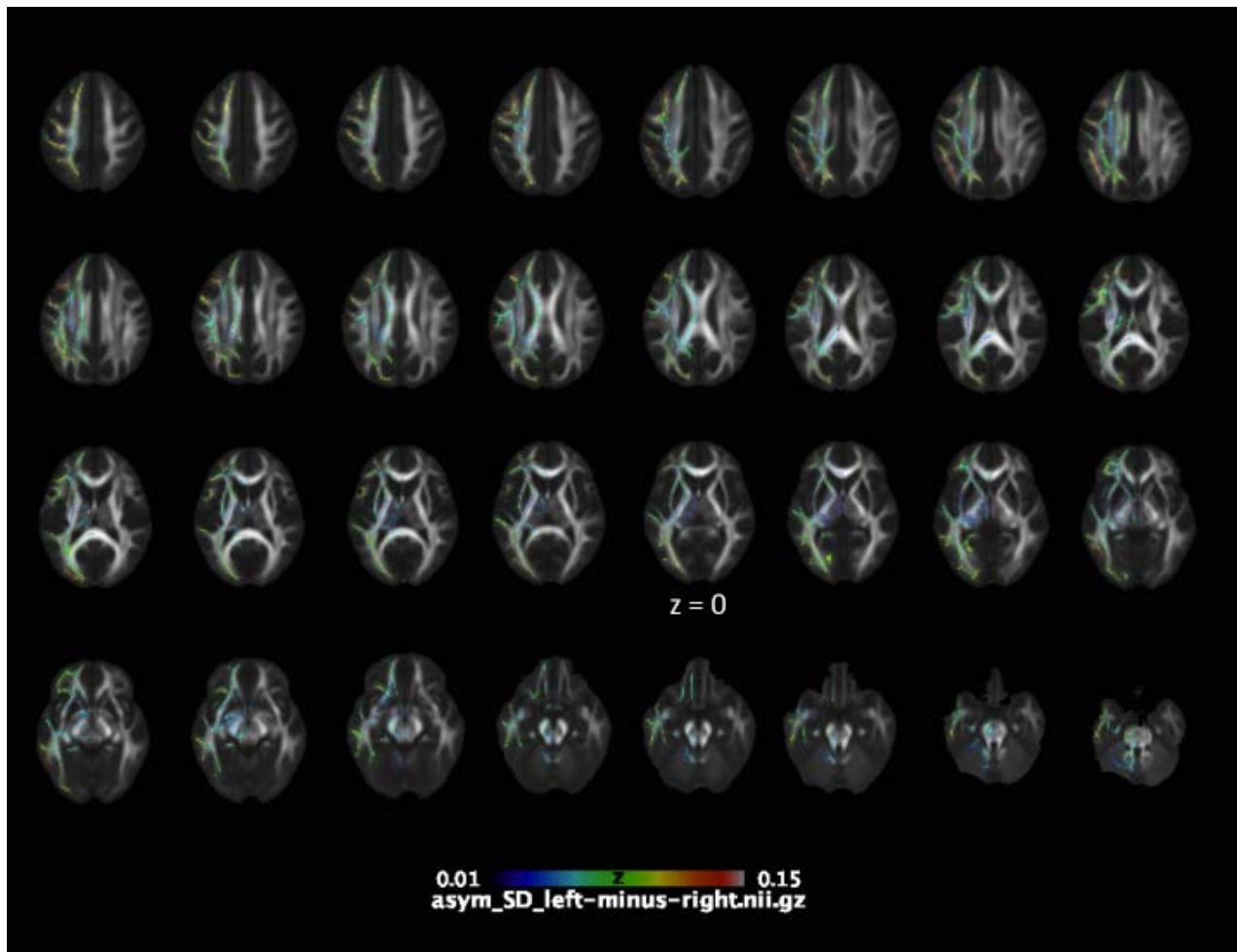
**Supplement Figure 4.** Lateralization pattern of white matter tract fractional anisotropy with tract-based spatial statistics in 5-year-olds. Significant regions with leftward asymmetry in red. Threshold-free cluster enhancement (TFCE) correction applied, 5000 permutations,  $p < 0.05$  (red colour bar showing  $p$  value). R = right, L = left



**Supplement Figure 5.** Mean values of lateralized FA (left minus right). Yellow to red colours (positive values) indicate leftward asymmetry and blue to green colours (negative values) rightward asymmetry.



**Supplement Figure 6.** Yellow to red colours (positive values) indicate leftward asymmetry and blue to green colours (negative values) rightward asymmetry.



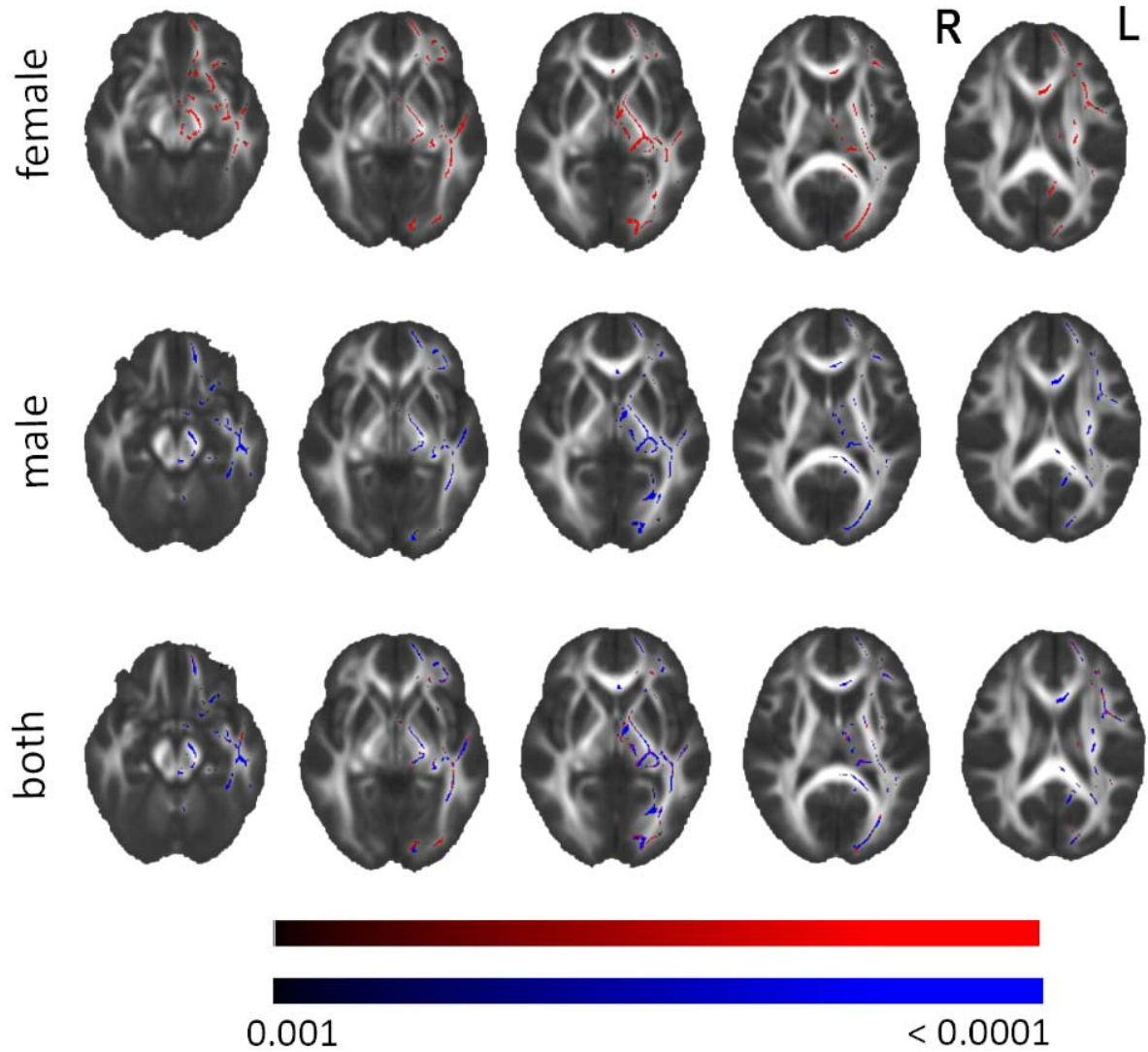
**Supplement Figure 7.** Inter-subject variation of lateralized FA values described as standard deviation (SD).

**Supplement Table 4.** Comparison of mean fractional anisotropy (FA) values in bilateral white matter tracts in 5-year-olds. CST = corticospinal tract, ML = medial lemniscus, ICP = inferior cerebellar peduncle, SCP = superior cerebellar peduncle, CP = cerebral peduncle, ALIC = anterior limb of internal capsule, PLIC = posterior limb of internal capsule, ACR = anterior corona radiata, SCR = superior corona radiata, PCR = posterior corona radiata, PTR (OR) = posterior thalamic radiation (optic tract), ILF/IFOF = inferior longitudinal fasciculus/inferior fronto-occipital fasciculus, EC = external capsule, CG = cingulate, CING = cingulum, ST = stria terminalis, SLF = superior longitudinal fasciculus, SFOF = superior fronto-occipital fasciculus, UNC = uncinata. Left-right difference of mean FA provided, negative values denote for rightward lateralization. Statistical significance calculated with one sample t test (two-tailed), Bonferroni corrected p value = 0.001 (0.05/36), tracts with significant difference in bold.

Tract		Mean FA	SD	Left-right difference	Sig.	Cohen's d																																																																																																																														
<b>CST</b>	right	<b>0,487</b>	<b>0,026</b>	<b>0,0194</b>	<b>0,000</b>	<b>0,721</b>																																																																																																																														
	left	<b>0,507</b>	<b>0,028</b>				<b>ALIC</b>	right	<b>0,544</b>	<b>0,024</b>	<b>-0,0224</b>	<b>0,000</b>	<b>0,903</b>	left	<b>0,521</b>	<b>0,025</b>	PLIC	right	0,653	0,020	0,0041	0,087	0,202	left	0,657	0,021	ACR	right	0,455	0,028	<b>-0,0077</b>	0,019	0,278	left	0,447	0,028	<b>SCR</b>	right	<b>0,467</b>	<b>0,025</b>	<b>0,0100</b>	<b>0,000</b>	<b>0,420</b>	left	0,477	0,023	PCR	right	0,440	0,027	<b>-0,0006</b>	0,843	0,023	left	0,439	0,028	PTR/OR	right	0,576	0,032	<b>-0,0002</b>	0,951	0,007	left	0,576	0,034	ILF/IFOF	right	0,507	0,028	0,0021	0,515	0,077	left	0,509	0,027	<b>EC</b>	right	<b>0,379</b>	<b>0,022</b>	<b>0,0220</b>	<b>0,000</b>	<b>1,00</b>	left	0,401	0,022	<b>CING</b>	right	<b>0,460</b>	<b>0,036</b>	<b>0,0256</b>	<b>0,000</b>	<b>0,700</b>	left	0,485	0,037	CG	right	0,408	0,038	0,0010	0,822	0,026	left	0,409	0,036	SLF	right	0,470	0,027	0,0027	0,403	0,099	left	0,473	0,027	<b>SFOF</b>	right	<b>0,475</b>	<b>0,039</b>	<b>-0,0281</b>	<b>0,000</b>	<b>0,706</b>	left	<b>0,447</b>	<b>0,041</b>	UNC	right	0,439	0,029	0,0106	0,003
<b>ALIC</b>	right	<b>0,544</b>	<b>0,024</b>	<b>-0,0224</b>	<b>0,000</b>	<b>0,903</b>																																																																																																																														
	left	<b>0,521</b>	<b>0,025</b>				PLIC	right	0,653	0,020	0,0041	0,087	0,202	left	0,657	0,021	ACR	right	0,455	0,028	<b>-0,0077</b>	0,019	0,278	left	0,447	0,028	<b>SCR</b>	right	<b>0,467</b>	<b>0,025</b>	<b>0,0100</b>	<b>0,000</b>	<b>0,420</b>	left	0,477	0,023	PCR	right	0,440	0,027	<b>-0,0006</b>	0,843	0,023	left	0,439	0,028	PTR/OR	right	0,576	0,032	<b>-0,0002</b>	0,951	0,007	left	0,576	0,034	ILF/IFOF	right	0,507	0,028	0,0021	0,515	0,077	left	0,509	0,027	<b>EC</b>	right	<b>0,379</b>	<b>0,022</b>	<b>0,0220</b>	<b>0,000</b>	<b>1,00</b>	left	0,401	0,022	<b>CING</b>	right	<b>0,460</b>	<b>0,036</b>	<b>0,0256</b>	<b>0,000</b>	<b>0,700</b>	left	0,485	0,037	CG	right	0,408	0,038	0,0010	0,822	0,026	left	0,409	0,036	SLF	right	0,470	0,027	0,0027	0,403	0,099	left	0,473	0,027	<b>SFOF</b>	right	<b>0,475</b>	<b>0,039</b>	<b>-0,0281</b>	<b>0,000</b>	<b>0,706</b>	left	<b>0,447</b>	<b>0,041</b>	UNC	right	0,439	0,029	0,0106	0,003	0,350	left	0,450	0,031						
PLIC	right	0,653	0,020	0,0041	0,087	0,202																																																																																																																														
	left	0,657	0,021				ACR	right	0,455	0,028	<b>-0,0077</b>	0,019	0,278	left	0,447	0,028	<b>SCR</b>	right	<b>0,467</b>	<b>0,025</b>	<b>0,0100</b>	<b>0,000</b>	<b>0,420</b>	left	0,477	0,023	PCR	right	0,440	0,027	<b>-0,0006</b>	0,843	0,023	left	0,439	0,028	PTR/OR	right	0,576	0,032	<b>-0,0002</b>	0,951	0,007	left	0,576	0,034	ILF/IFOF	right	0,507	0,028	0,0021	0,515	0,077	left	0,509	0,027	<b>EC</b>	right	<b>0,379</b>	<b>0,022</b>	<b>0,0220</b>	<b>0,000</b>	<b>1,00</b>	left	0,401	0,022	<b>CING</b>	right	<b>0,460</b>	<b>0,036</b>	<b>0,0256</b>	<b>0,000</b>	<b>0,700</b>	left	0,485	0,037	CG	right	0,408	0,038	0,0010	0,822	0,026	left	0,409	0,036	SLF	right	0,470	0,027	0,0027	0,403	0,099	left	0,473	0,027	<b>SFOF</b>	right	<b>0,475</b>	<b>0,039</b>	<b>-0,0281</b>	<b>0,000</b>	<b>0,706</b>	left	<b>0,447</b>	<b>0,041</b>	UNC	right	0,439	0,029	0,0106	0,003	0,350	left	0,450	0,031																
ACR	right	0,455	0,028	<b>-0,0077</b>	0,019	0,278																																																																																																																														
	left	0,447	0,028				<b>SCR</b>	right	<b>0,467</b>	<b>0,025</b>	<b>0,0100</b>	<b>0,000</b>	<b>0,420</b>	left	0,477	0,023	PCR	right	0,440	0,027	<b>-0,0006</b>	0,843	0,023	left	0,439	0,028	PTR/OR	right	0,576	0,032	<b>-0,0002</b>	0,951	0,007	left	0,576	0,034	ILF/IFOF	right	0,507	0,028	0,0021	0,515	0,077	left	0,509	0,027	<b>EC</b>	right	<b>0,379</b>	<b>0,022</b>	<b>0,0220</b>	<b>0,000</b>	<b>1,00</b>	left	0,401	0,022	<b>CING</b>	right	<b>0,460</b>	<b>0,036</b>	<b>0,0256</b>	<b>0,000</b>	<b>0,700</b>	left	0,485	0,037	CG	right	0,408	0,038	0,0010	0,822	0,026	left	0,409	0,036	SLF	right	0,470	0,027	0,0027	0,403	0,099	left	0,473	0,027	<b>SFOF</b>	right	<b>0,475</b>	<b>0,039</b>	<b>-0,0281</b>	<b>0,000</b>	<b>0,706</b>	left	<b>0,447</b>	<b>0,041</b>	UNC	right	0,439	0,029	0,0106	0,003	0,350	left	0,450	0,031																										
<b>SCR</b>	right	<b>0,467</b>	<b>0,025</b>	<b>0,0100</b>	<b>0,000</b>	<b>0,420</b>																																																																																																																														
	left	0,477	0,023				PCR	right	0,440	0,027	<b>-0,0006</b>	0,843	0,023	left	0,439	0,028	PTR/OR	right	0,576	0,032	<b>-0,0002</b>	0,951	0,007	left	0,576	0,034	ILF/IFOF	right	0,507	0,028	0,0021	0,515	0,077	left	0,509	0,027	<b>EC</b>	right	<b>0,379</b>	<b>0,022</b>	<b>0,0220</b>	<b>0,000</b>	<b>1,00</b>	left	0,401	0,022	<b>CING</b>	right	<b>0,460</b>	<b>0,036</b>	<b>0,0256</b>	<b>0,000</b>	<b>0,700</b>	left	0,485	0,037	CG	right	0,408	0,038	0,0010	0,822	0,026	left	0,409	0,036	SLF	right	0,470	0,027	0,0027	0,403	0,099	left	0,473	0,027	<b>SFOF</b>	right	<b>0,475</b>	<b>0,039</b>	<b>-0,0281</b>	<b>0,000</b>	<b>0,706</b>	left	<b>0,447</b>	<b>0,041</b>	UNC	right	0,439	0,029	0,0106	0,003	0,350	left	0,450	0,031																																				
PCR	right	0,440	0,027	<b>-0,0006</b>	0,843	0,023																																																																																																																														
	left	0,439	0,028				PTR/OR	right	0,576	0,032	<b>-0,0002</b>	0,951	0,007	left	0,576	0,034	ILF/IFOF	right	0,507	0,028	0,0021	0,515	0,077	left	0,509	0,027	<b>EC</b>	right	<b>0,379</b>	<b>0,022</b>	<b>0,0220</b>	<b>0,000</b>	<b>1,00</b>	left	0,401	0,022	<b>CING</b>	right	<b>0,460</b>	<b>0,036</b>	<b>0,0256</b>	<b>0,000</b>	<b>0,700</b>	left	0,485	0,037	CG	right	0,408	0,038	0,0010	0,822	0,026	left	0,409	0,036	SLF	right	0,470	0,027	0,0027	0,403	0,099	left	0,473	0,027	<b>SFOF</b>	right	<b>0,475</b>	<b>0,039</b>	<b>-0,0281</b>	<b>0,000</b>	<b>0,706</b>	left	<b>0,447</b>	<b>0,041</b>	UNC	right	0,439	0,029	0,0106	0,003	0,350	left	0,450	0,031																																														
PTR/OR	right	0,576	0,032	<b>-0,0002</b>	0,951	0,007																																																																																																																														
	left	0,576	0,034				ILF/IFOF	right	0,507	0,028	0,0021	0,515	0,077	left	0,509	0,027	<b>EC</b>	right	<b>0,379</b>	<b>0,022</b>	<b>0,0220</b>	<b>0,000</b>	<b>1,00</b>	left	0,401	0,022	<b>CING</b>	right	<b>0,460</b>	<b>0,036</b>	<b>0,0256</b>	<b>0,000</b>	<b>0,700</b>	left	0,485	0,037	CG	right	0,408	0,038	0,0010	0,822	0,026	left	0,409	0,036	SLF	right	0,470	0,027	0,0027	0,403	0,099	left	0,473	0,027	<b>SFOF</b>	right	<b>0,475</b>	<b>0,039</b>	<b>-0,0281</b>	<b>0,000</b>	<b>0,706</b>	left	<b>0,447</b>	<b>0,041</b>	UNC	right	0,439	0,029	0,0106	0,003	0,350	left	0,450	0,031																																																								
ILF/IFOF	right	0,507	0,028	0,0021	0,515	0,077																																																																																																																														
	left	0,509	0,027				<b>EC</b>	right	<b>0,379</b>	<b>0,022</b>	<b>0,0220</b>	<b>0,000</b>	<b>1,00</b>	left	0,401	0,022	<b>CING</b>	right	<b>0,460</b>	<b>0,036</b>	<b>0,0256</b>	<b>0,000</b>	<b>0,700</b>	left	0,485	0,037	CG	right	0,408	0,038	0,0010	0,822	0,026	left	0,409	0,036	SLF	right	0,470	0,027	0,0027	0,403	0,099	left	0,473	0,027	<b>SFOF</b>	right	<b>0,475</b>	<b>0,039</b>	<b>-0,0281</b>	<b>0,000</b>	<b>0,706</b>	left	<b>0,447</b>	<b>0,041</b>	UNC	right	0,439	0,029	0,0106	0,003	0,350	left	0,450	0,031																																																																		
<b>EC</b>	right	<b>0,379</b>	<b>0,022</b>	<b>0,0220</b>	<b>0,000</b>	<b>1,00</b>																																																																																																																														
	left	0,401	0,022				<b>CING</b>	right	<b>0,460</b>	<b>0,036</b>	<b>0,0256</b>	<b>0,000</b>	<b>0,700</b>	left	0,485	0,037	CG	right	0,408	0,038	0,0010	0,822	0,026	left	0,409	0,036	SLF	right	0,470	0,027	0,0027	0,403	0,099	left	0,473	0,027	<b>SFOF</b>	right	<b>0,475</b>	<b>0,039</b>	<b>-0,0281</b>	<b>0,000</b>	<b>0,706</b>	left	<b>0,447</b>	<b>0,041</b>	UNC	right	0,439	0,029	0,0106	0,003	0,350	left	0,450	0,031																																																																												
<b>CING</b>	right	<b>0,460</b>	<b>0,036</b>	<b>0,0256</b>	<b>0,000</b>	<b>0,700</b>																																																																																																																														
	left	0,485	0,037				CG	right	0,408	0,038	0,0010	0,822	0,026	left	0,409	0,036	SLF	right	0,470	0,027	0,0027	0,403	0,099	left	0,473	0,027	<b>SFOF</b>	right	<b>0,475</b>	<b>0,039</b>	<b>-0,0281</b>	<b>0,000</b>	<b>0,706</b>	left	<b>0,447</b>	<b>0,041</b>	UNC	right	0,439	0,029	0,0106	0,003	0,350	left	0,450	0,031																																																																																						
CG	right	0,408	0,038	0,0010	0,822	0,026																																																																																																																														
	left	0,409	0,036				SLF	right	0,470	0,027	0,0027	0,403	0,099	left	0,473	0,027	<b>SFOF</b>	right	<b>0,475</b>	<b>0,039</b>	<b>-0,0281</b>	<b>0,000</b>	<b>0,706</b>	left	<b>0,447</b>	<b>0,041</b>	UNC	right	0,439	0,029	0,0106	0,003	0,350	left	0,450	0,031																																																																																																
SLF	right	0,470	0,027	0,0027	0,403	0,099																																																																																																																														
	left	0,473	0,027				<b>SFOF</b>	right	<b>0,475</b>	<b>0,039</b>	<b>-0,0281</b>	<b>0,000</b>	<b>0,706</b>	left	<b>0,447</b>	<b>0,041</b>	UNC	right	0,439	0,029	0,0106	0,003	0,350	left	0,450	0,031																																																																																																										
<b>SFOF</b>	right	<b>0,475</b>	<b>0,039</b>	<b>-0,0281</b>	<b>0,000</b>	<b>0,706</b>																																																																																																																														
	left	<b>0,447</b>	<b>0,041</b>				UNC	right	0,439	0,029	0,0106	0,003	0,350	left	0,450	0,031																																																																																																																				
UNC	right	0,439	0,029	0,0106	0,003	0,350																																																																																																																														
	left	0,450	0,031																																																																																																																																	





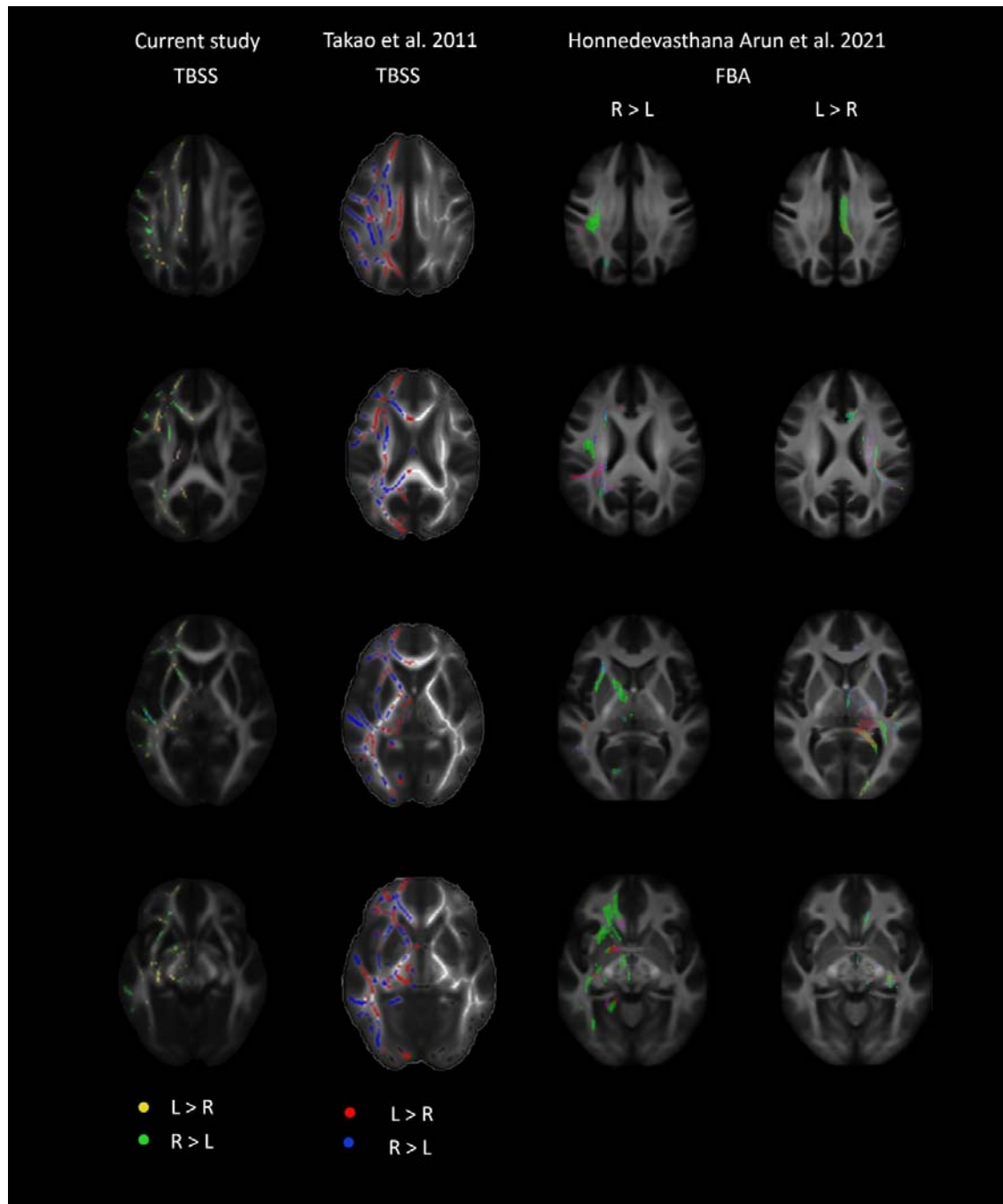


**Supplement Figure 8.** Sex-specific white matter lateralization patterns of 5-year-olds with Tract-based Spatial Statistical (TBSS) analysis, depicted as left-right fractional anisotropy values. The statistically significantly asymmetric regions showed with red in females and with blue in males. Analyses conducted with 5000 permutations, threshold-free cluster enhancement (TFCE) correction applied,  $p < 0.001$ . R = right, L = left

**Supplement Table 5.** Mean fractional anisotropy (FA) and standard deviation (SD) of each white matter tract in infants and in 5-year-olds. GCC = genu of corpus callosum, BCC = body of corpus callosum, SCC = splenium of corpus callosum, CST = corticospinal tract, ICP = inferior cerebellar peduncle, SCP = superior cerebellar peduncle, CP = cerebral peduncle, ALIC = anterior limb of internal capsule, PLIC = posterior limb of internal capsule, rI IC = retrolenticular internal capsule, ACR = anterior corona radiata, SCR = superior corona radiata, PCR = posterior corona radiata, PTR (OR) = posterior thalamic radiation (optic tract), ILF/IFOF = inferior longitudinal fasciculus/inferior fronto-occipital fasciculus, EC = external capsule, CG = cingulate, CING = cingulum, ST = stria terminalis, SLF = superior longitudinal fasciculus, SFOF = superior fronto-occipital fasciculus, UNC = uncinata, R = right, L = left.

	infants		5-year-olds	
	FA	SD	FA	SD
GCC	0.33	0.029	0.72	0.035
BCC	0.31	0.026	0.64	0.038
SCC	0.39	0.032	0.74	0.028
Fornix	0.24	0.020	0.45	0.042
CST R	0.24	0.024	0.49	0.026
CST L	0.24	0.027	0.51	0.028
ICP R	0.20	0.020	0.47	0.028
ICP L	0.21	0.026	0.47	0.024
SCP R	0.27	0.024	0.57	0.028
SCP L	0.32	0.028	0.60	0.028
CP R	0.31	0.023	0.63	0.024
CP L	0.32	0.027	0.64	0.024
ALIC R	0.29	0.020	0.54	0.024
ALIC L	0.26	0.020	0.52	0.025
PLIC R	0.39	0.024	0.65	0.020
PLIC L	0.38	0.024	0.66	0.021
rI IC R	0.38	0.024	0.54	0.028
rI IC L	0.36	0.022	0.56	0.024
ACR R	0.22	0.026	0.46	0.028
ACR L	0.22	0.025	0.45	0.028
SCR R	0.29	0.022	0.47	0.025
SCR L	0.28	0.021	0.48	0.023
PCR R	0.25	0.025	0.44	0.027
PCR L	0.27	0.026	0.44	0.028
PTR/OR R	0.31	0.024	0.58	0.032
PTR/OR L	0.32	0.026	0.58	0.034
ILF/IFOF R	0.29	0.027	0.51	0.028
ILF/IFOF L	0.30	0.027	0.51	0.027
EC R	0.24	0.017	0.38	0.022
EC L	0.25	0.017	0.40	0.022
CG R	0.25	0.043	0.46	0.036
CG L	0.27	0.035	0.49	0.037
CING R	0.19	0.026	0.41	0.038
CING L	0.20	0.026	0.41	0.036
Fornix/ST R	0.26	0.021	0.51	0.029
Fornix/ST L	0.31	0.023	0.52	0.028
SLF R	0.23	0.023	0.47	0.027
SLF L	0.24	0.022	0.47	0.027
SFOF R	0.34	0.030	0.48	0.039
SFOF L	0.19	0.020	0.45	0.041

UNC R	0.30	0.045	0.44	0.029
UNC L	0.26	0.051	0.45	0.031



**Supplement Figure 9.** Comparison of lateralization patterns in our study and two previously published adult-population studies (Takao et al. 2011 and Honnedevasathana Arun et al. 2021). Figure adapted from previously published figures by Takao et al. 2011<sup>1</sup> and Honnedevasathana Arun et al. 2021<sup>2</sup>, Copyright Elsevier. TBSS = tract-based spatial statistics, FBA = fixel-based analysis, L = left, R = right

1. Takao, H., Hayashi, N., & Ohtomo, K. (2011). White matter asymmetry in healthy individuals: A diffusion tensor imaging study using tract-based spatial statistics. *Neuroscience*, 193, 291–299. <https://doi.org/10.1016/j.neuroscience.2011.07.041>
2. Honnedevassthana Arun, A., Connelly, A., Smith, R. E., & Calamante, F. (2021). Characterisation of white matter asymmetries in the healthy human brain using diffusion MRI fixel-based analysis. *NeuroImage*, 225(November 2020), 117505. <https://doi.org/10.1016/j.neuroimage.2020.117505>